EVALUATION OF SKYLAB PHOTOGRAPHS

FOR MAPPING QUATERNARY GEOLOGIC FEATURES,

WEST-CENTRAL SMOKE CREEK DESERT, NEVADA

by

Rebecca L. Dodge

ProQuest Number: 10782153

ProQuest 10782153

Published by ProQuest LLC (2018). Copyright of the Dissertation is held by the Author.

ProQuest LLC.
789 East Eisenhower Parkway
P.O. Box 1346
Ann Arbor, MI 48106 – 1346

A Thesis submitted to the Faculty and the Board of
Trustees of the Colorado School of Mines in partial ful-
fillment of the requirements for the degree of Master of
Science (Geology).

Signed: _____
Student
Rebecca L. Dodge

Golden, Colorado

Date: _____, 1978

Approved: _____
Thesis Advisor
Dr. Keenan Lee

_____
Head of Department
Dr. J. Finney

Golden, Colorado

Date: _____, 1978

ii

ABSTRACT

Skylab photographs are a good base for mapping faults and surface units, and a good guide to possible spring locations, in the arid terrain typical of northwest Nevada deserts. Vegetation differences along and on opposite sides of faults are the best fault indicators. Vegetation associated with springs is the best guide to spring location, and texture and color are most important in separating surface units. In the west-central Smoke Creek Desert, all Quaternary faults except one were interpreted as probable faults on the Skylab S190B photographs, and all springs associated with faulting were interpreted as probable springs on S190A photographs. Five of seven major surface units were mapped accurately on S190B photographs.

The west-central Smoke Creek Desert is part of a broad area of the western United States that is undergoing east-west crustal extension and normal faulting. It is separated from similar normal-faulted areas to the north and south by northwest-trending right-lateral strike-slip fault zones. Movement on these zones compensates for differential extension between the west-central Smoke Creek Desert area and areas to the north and south. Modern seismicity suggests that active faulting is presently concentrated along the strike-slip zones, while normal fault movement in the area

between the two zones is less active.

TABLE OF CONTENTS

ILLUSTRATIONS

Figure		Page

TABLES

ix

ACKNOWLEDGEMENTS

INTRODUCTION

OBJECTIVE

The objective of this research was to evaluate the utility of Skylab orbital photography for mapping Quaternary geologic features in the Basin and Range province of western North America. Emphasis was placed on mapping Holocene faulting and spring activity, which might serve as indicators of geothermal activity. Mapping surface units received secondary emphasis. Most of the geology of northwestern Nevada has been mapped only at a scale of 1:250,000. It was hoped that more detailed and larger scale mapping could be accomplished through photointerpretation of Skylab photographs, complemented by field checking. The west-central Smoke Creek Desert was chosen as the site for large-scale mapping.

LOCATION AND GEOLOGIC SETTING

The Smoke Creek Desert is a north to northeast-trending basin, a graben, in northwestern Nevada. The field area is outlined on figure 1. The southern tip of the basin is 50 miles (80 km) north of Reno, Nevada, and about 5 miles (8 km) northwest of Pyramid Lake. The basin is about 40 miles (64 km) long and no greater than 15 miles (24 km) wide. Access is by graded gravel road that runs along the western margin of the basin. Unimproved dirt roads provide limited lateral access.
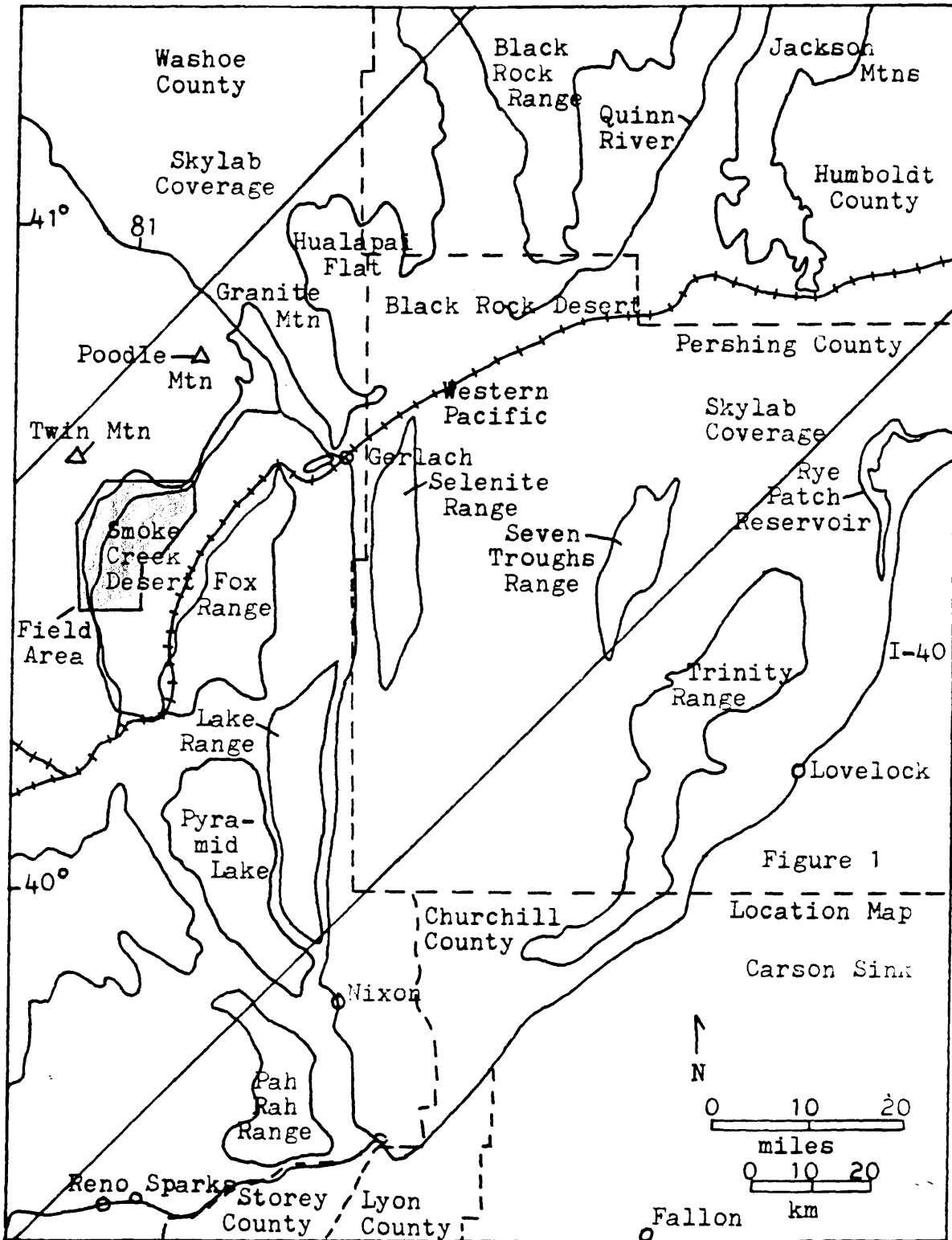
Figure 1. Location Map

The Smoke Creek Desert is in the northwestern Great
Basin section of the Basin and Range province (fig. 2).
More specifically, it is within the Lahonton Basin, a major
low area of internal drainage within the Great Basin. To
the north and west, the Smoke Creek Desert is bounded by the
elevated, block-faulted Modoc Plateau, which is composed of
Tertiary volcanic flows, pyroclastic rocks, and tuffaceous
sedimentary rocks ranging in age from Oligocene to Pliocene.
Several shield volcanoes are scattered through the Plateau.
Three large north-trending, en echelon, normal faults form
the boundary between the Smoke Creek Desert and the Modoc
Plateau. The 'most recent movement on these faults took place
during the early or middle Pleistocene (MacDonald, 1966).
Other faults in the Modoc Plateau are Pleistocene to Holocene
in age and trend north to northwest. MacDonald (1966) found
most of the movement along these faults to be dip-slip, with
little evidence of a strike-slip component. An exception is
the Likely fault, a northwest-trending, right-slip fault (fig.
2).

To the east of the Smoke Creek Desert, the Great Basin
is characterized by steeply-dipping normal faults that form
a system of north- to northeast-trending horsts and grabens
(Wright, 1976). The individual fault blocks are tilted gently
eastward or westward (Wright, 1976). To the south of the
Smoke Creek Desert, gently dipping normal faults, trending
north to northeast, bound steeply-tilted blocks in a horst
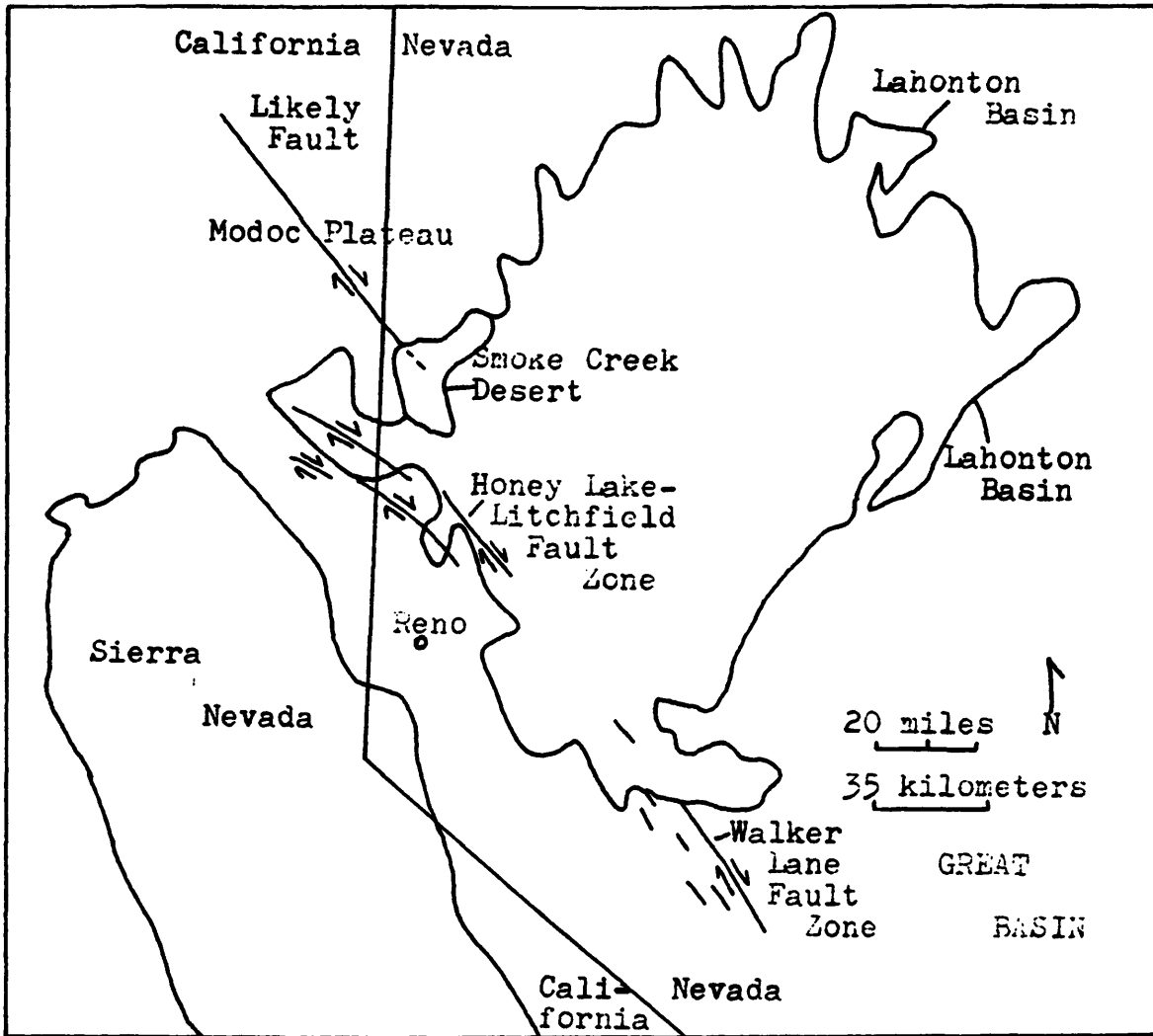
Figure 2. Geologic setting of the Smoke Creek Desert

and graben system (Wright, 1976). Northwest-trending, right-slip faults separate this part of the Great Basin from the area to the north and east (Wright, 1976). Two of the larger strike-slip fault zones are the Walker Lane and Honey Lake-Litchfield zones (fig. 2, p. 4).

CLIMATE AND VEGETATION

The climate of the Smoke Creek Desert is arid and cool. Summers are warm, with a mean temperature in July of about $67^\circ F$ ($20^\circ C$). Winters are cool, with a mean temperature of about $30^\circ F$ ($-1^\circ C$). Annual precipitation is between 7 and 10 inches (18-25 cm), increasing with altitude. The altitude in the field area ranges from 3900 to 4700 feet (1190 to 1433 m).

Most of the field area is covered with phreatophytes such as rabbitbrush (Chrysothamnus nauseosus) and bitterbrush (Purshia tridentata), and the xerophyte Basin sagebrush (Artemisia tridentata). Vegetation was of great value in this research because it is closely controlled by the availability of water. An abundant, year-round supply of surface water is available only in a few areas of the Smoke Creek Desert. The drainage of the Smoke Creek (see Plate 1, in pocket) contains water all year; the only other surface water is in springs and seeps. Although there are a few springs present where deflation or stream erosion has reached the water table, most of the springs and seeps are found along

Holocene faults. In these areas the phreatophytes grow much denser and larger, and trees such as cottonwood (Populus fremontii) and aspen (Populus tremuloides) are sometimes present. These vegetation "anomalies" serve to highlight the faults dramatically (fig. 3).

SKYLAB SYSTEM

The statistics in the following discussion are from the photography catalog for Skylab 3, from the University of New Mexico Technology Application Center. The photography used in this research was obtained during the Skylab 3 orbital mission. The Skylab 3 crew manned the laboratory between July 28 and September 25, 1973, orbiting the earth every 93 minutes at an altitude of 272 miles (434 km). The area of study was photographed simultaneously by both the S190A multispectral camera and the S190B high resolution earth terrain camera in September (fig. 1).

The S190A camera consisted of six 6-inch focal length lenses which photographed the same scene simultaneously, using six different film and filter combinations. Coverage is available in black and white of two infrared bands (0.7-0.8μm and 0.8-0.9μm) and two visible bands (0.5-0.6μm, green, and 0.6-0.7μm, red). Color infrared photography (0.5-0.88μm) and color photography (0.4-0.7μm) are also available. The S190B camera had one 18-inch focal length lens, and color film was used in the flight over the field

Figure 3. Anomalously dense vegetation highlights
a Holocene fault in the west-central Smoke Creek
Desert. Aerial view towards the east of fault F
(see Plate 1, in pocket).

area.

Stereo photographic coverage was obtained over the northwest Nevada area from the S190A system in color, color infrared, and black and white (red band). The photographs are in 9x9-inch transparency format (3x enlargements, 3rd generation), with a scale of approximately 1:950,000. Each frame is 101 statute miles (162 km) on a side. The resolution of the color film is approximately 80 feet (55 m), and that of the red band approximately 90 feet (27 m). The S190B photographs, also in stereo, are in 9x9-inch transparency format (2x enlargements, 3rd generation), with a scale of approximately 1:475,000. Each frame covers 68x68 miles (109x109 km). The color film has a resolution of approximately 60 feet (20 m).

PREVIOUS WORK

Northern Nevada Geothermal Systems

Geologic controls of Basin and Range geothermal systems were studied by R.K. Hose and B.E. Taylor of the U.S.G.S. between 1972 and 1974 (Hose and Taylor, 1974). The authors concluded that geothermal systems exist because meteoric waters circulate to significant depths (up to 3 km) in the valley-fill sediments and are heated by high heat flow from the mantle through the thinned crust under northern Nevada. Wollenberg and others' (1975) research in northern Nevada concluded that fault zones furnish "permeable pathways for

downward percolating meteoric water to reach sufficient
depth (4-5 km) in a region of high geothermal gradient...",
as well as "channelways for upward transport of hot waters."
Grose and Keller (1976, personal communication) also emphasize
the importance of faulting in localization of geothermal acti-
vity, based on studies conducted in the Black Rock Desert
of northern Nevada. The longevity of geothermal systems may
be controlled by repeated fracturing along active faults,
which maintains permeability in the system. Recognition of
Holocene faulting seems to be an important criterion in geo-
thermal exploration. Therefore, special emphasis was placed
on recognition of Holocene faults in this research.

Skylab Photography Applications

Faculty and students of the Colorado School of Mines
have recently completed an extensive evaluation of Skylab
photography over Colorado for geologic mapping, mineral re-
sources exploration, and water resources studies (Lee and
others, 1975). Conclusions on the utility of Skylab photo-
graphy for interpretation of geologic structure are that
fractures as short as one kilometer can be detected on the
high-resolution S109B photography, and two-kilometer-long
fractures can be mapped on the lower-resolution S190A
photography.

Researchers in southern California have recently com-
pleted studies on the utility of Skylab photography for

interpreting fault tectonics. Investigations in the Salton
Trough area (Merifield and Lamar, 1975a) revealed features
visible on Skylab photographs that are distinctive of active
faults, including scarps, offset drainages, and vegetation
differences in alluvium controlled by ground water blockage.
Further research in the Peninsular Ranges of southwestern
California (Lamar and Merifield, 1975), using Landsat and
Skylab, revealed several linears that were identified as
faults previously unrecognized by field investigators. The
authors reiterated their conclusion that regional fault in-
vestigations should begin with the study of satellite images,
and they emphasized the utility "of the higher-resolution
Skylab imagery in distinguishing active from inactive faults".

Abdel-Gawad and Tubbesing (1975) used Skylab photography
to study faults and "tectonic lines" in selected areas of the
U.S. Southwest. They concluded that "image quality and
ground resolution are sufficient to identify many geomorphic
features associated with recent faulting."

The optimum scale for geologic mapping with Skylab
S190B photographs was determined to be about 1:62,500 for an
area aroung Moab, Utah (Lee and Weimer, 1975). Optimum map-
ping scale for S190A photography would be smaller because of
its inherently smaller scale.

Geologic Mapping

Geologic maps of the region include those by Bonham

(1969) of Washoe and Storey Counties, Nevada, by Tatlock

(1969) of Pershing County, Nevada, and by Willden (1964) of

Humboldt County, Nevada, all to a scale of 1:250,000. To

the west and northwest in California, are the Westwood (Susan-

ville) sheet by Lydon, Gay and Jennings (1960) and the

Alturas sheet by Gay and Aune (1958), both to a scale of

1:250,000. Larger scale geologic maps of several areas to

the north and northeast of the Smoke Creek Desert have been

compiled under the auspices of the Colorado School of Mines

Nevada Geothermal Study. Summaries of these works are

available in Grose and Keller (1974, 1975).

GEOLOGY OF THE WEST-CENTRAL

SMOKE CREEK DESERT

GEOLOGIC FORMATIONS

With the exception of a 1-square-mile (2.5 sq. km)

outcrop of Cretaceous granodiorite, the entire field area is

covered by Cenozoic volcanic and nonmarine sedimentary rocks,

including lacustral and alluvial deposits. About 80% of the

area is mantled by Quaternary sediments. In the remaining

area upper Miocene and Pliocene volcanic flows and volcanic

sediments, mostly basalts and tuffs, crop out. Plate 1 (in

pocket) is a geologic map of the west-central Smoke Creek

Desert.

Mesozoic Rocks

Cretaceous Intrusive Rock (Kgd)

This unit has no formal name and is usually called

"Cretaceous granodiorite" in the literature (Bonham, 1969).

The granodiorite is in intrusive contact with metamorphosed

Permo-Triassic rocks to the north of the field area. It is

nonconformably overlain by the Tertiary High Rock sequence

and Pleistocene Lake Lahonton sediments in the field area.

Lithology: The Cretaceous intrusive is a grey, equi-

granular, medium-grained hornblende-biotite granodiorite.

Mafic minerals compose about 20% of the rock, with biotite

content slightly higher than hornblende. Accessories include

sphene, magnetite, and zircon. About 40% of the rock is
plagioclase, 25% quartz, and 14% alkali feldspar.

Correlation and Age: Smith and others (1971) age dated
twenty-six granitic plutons in northwestern Nevada, including
the Granite Range pluton and the Selenite Range pluton (see
fig. 1, p. 2). The plutons range in age from 175 to 85 mil-
lion years old, but most are between 105 and 85 million years
old. On the basis of age and petrographic and chemical
affinities these authors correlated the northwestern Nevada
granitic plutons with those of the Sierra Nevada and Idaho
batholiths.

Cenozoic Rocks

Canyon Assemblage

Two units of the Canyon Assemblage, described by Bonham
in 1969, crop out in the west-central Smoke Creek Desert.
The High Rock sequence (Tts) outcrop covers about 3 square
miles in the northeast corner of the field area, and upper
Miocene and Pliocene basalts (Tba) crop out on the western
edge of the field area.

The High Rock sequence, as informally named by Bonham
(1969), comprises an areally extensive and variable group of
ash-flow tuffs, fluviolacustral sedimentary rocks, mafic
tuffs, and lava flows. Bonham defined this diverse lithologic
sequence as a "stratigraphic unit bounded by distinct changes
in lithology and commonly by unconformities at its base and

top". The High Rock sequence in the west-central Smoke

Creek Desert overlies Cretaceous granodiorite (Kgd) noncon-

formably, and is disconformably overlain by upper Miocene and

Pliocene basalts (Tba).

Lithology: The High Rock sequence in the field area is

a thinly to thickly bedded, fluviolacustral, tuffaceous sedi-

mentary rock composed of a mixture of pyroclastic and sedi-

mentary detritus. It varies in color from pale buff to

light yellowish brown. Fragmental constituents are sand to

pebble-size basalt, basalt porphyry, and tuffaceous material

in a tuffaceous matrix (fig. 4). Locally, large (15-40 inches,

38-100 cm) blocks of pumice are present within the sediments.

Several small basaltic dikes intrude the unit within the field

area, and probably represent feeder dikes for the overlying

basalts (Bonham, 1969).

The dip of the sequence in the field area varies from

nearly horizontal to greater than 20° within the three-square-

mile outcrop. This variation may be tectonic in origin, re-

lated to Basin and Range faulting, or it may be related to

post-depositional slumping of water-saturated sediments in a

fluviolacustral environment as suggested by Bonham in 1969.

Because of limited exposure in the west-central Smoke Creek

Desert, the exact cause of deformation is not discernible.

Correlation and Age: The High Rock sequence of north-

west Nevada is correlated by Bonham (1969) with similar vol-

canic sedimentary rocks of late Miocene and Pliocene age in

Figure 4. The High Rock Sequence (Tts), a tuffa-
ceous sedimentary rock.

California and Oregon. Age dates have been obtained from
both vertebrate fossils and potassium-argon dating of rocks.
This areally extensive sequence is generally correlated on
the basis of similar lithologies and stratigraphic position
rather than by actual continuity of single units over broad
areas.

Bonham (1969) proposes no formal name for the sequence
of basalt flows overlying the High Rock sequence in northwest
Nevada, and declines to apply names given areally coextensive
basalt formations in California and Oregon. The basalts form
the upper part of the Canyon Assemblage, and are here called
simply "upper Miocene and Pliocene basalts". This designa-
tion covers a series of basalts erupted discontinuously from
numerous vents and fissures onto an eroded surface of the
High Rock sequence. The disconformable contact between the
two is essentially concordant, indicating that little struc-
tural deformation took place between deposition of the two
units.

The basalts in the field area are nearly flat-lying,
except where they have been gently tilted westward by Basin
and Range normal faulting of late Pliocene to early Pleisto-
cene age. Twin Mountain (fig. 1, p. 2), a 6,605 foot (2013 m)
peak to the northwest of the field area, is an eroded shield
volcano (Bonham, 1969) that may be the source of the basalts
in the field area. Other smaller vents and now-buried fissures
may have contributed to the basalt accumulation.

Lithology: The flows consist of olivine basalts. A

typical sample has an intergranular texture and is composed

of 20% olivine, 10% olivine altered to iddingsite, 10% augite,

and 2% sphene, in a matrix of 40% plagioclase and 10% glassy

material. Hematite and magnetite are accessory constituents.

Individual flows commonly have scoriaceous tops and bottoms,

and microvesicular interiors.

Two minor non-basaltic members of the upper Miocene and

Pliocene basalt crop out in the west-central Smoke Creek

Desert. The unit designated Tbp is a small (2000 feet or

610 m in diameter), nearly circular breccia pipe intruded

near the east-central margin of the basalts (see Plate 1 and

Figures 5 and 6). This intrusion consists of mineral frag-

ments of plagioclase and biotite, and lithic fragments of

basalt, olivine basalt, and andesite. The lithic fragments

range in size from pebbles to boulders, and are embedded in

a matrix of buff-colored amorphous material. The intrusion

was emplaced before normal faulting of the western edge of

the Smoke Creek Desert (late Pliocene or early Pleistocene).

The unit designated Tbt (fig. 7, p. 19) consists of a

group of thinly-bedded tuffaceous sedimentary rocks of un-

known thickness (maximum exposure, 18 feet or 5.5 m) that

has been exposed by erosion of a downfaulted block of the

basalts. It has very limited exposure because it is covered

by Quaternary lake beds. Individual beds within the unit

include minor thin ash falls and a mud flow, but are
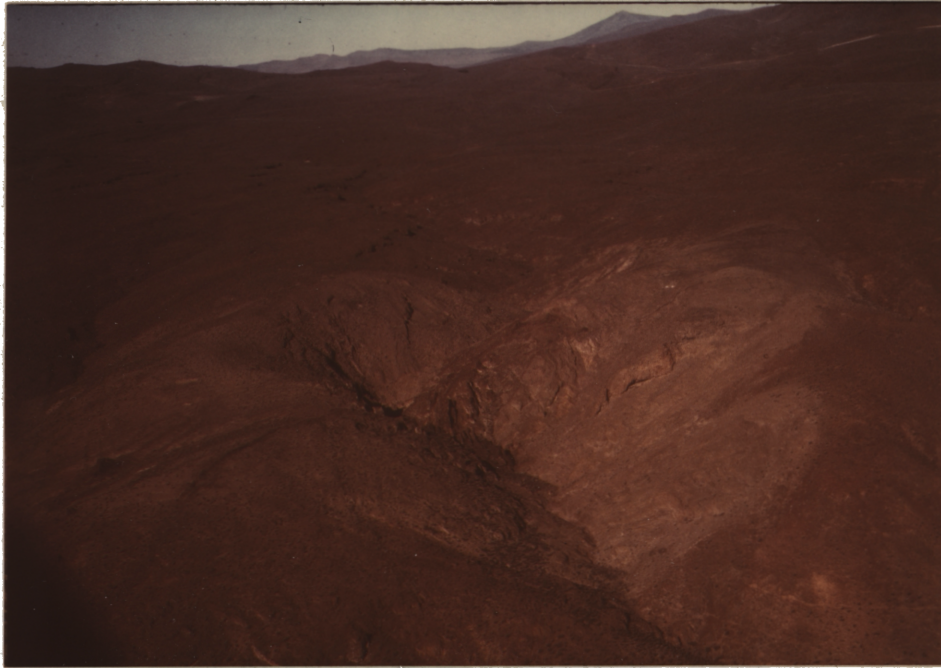
Figure 5. Aerial view, looking west, of breccia pipe (Tbp) intruding basalt (Tba). The intrusion is approximately 2000 feet (610 m) in diameter.

Figure 6. Breccia pipe (Tbp) consisting of basalt, andesite, plagioclase, and biotite fragments in an amorphous matrix.

Figure 7. Contact between the basalts (Tba) and the
intercalated tuffaceous sedimentary unit (Tbt).

predominantly interbedded cross-stratified sandstone and siltstones composed of volcanic rock fragments and tuffaceous material. The unit is interpreted as fluviolacustral in origin.

Correlation and Age: The upper Miocene and Pliocene basalt flows of northwestern Nevada are coextensive and in part correlative with the Mesa Basalt Formation of Merriam (1959) and the "Warner" Basalt Formation of Russell (1928). Bonham (1969) suggests that neither formational name is applicable to the northwestern Nevada basalt because 1) the Warner Basalt includes flows ranging from early Miocene to Pleistocene in age, and 2) the name Mesa Basalt was originally applied to flows more than 100 miles (160 km) away.

Part of the upper Miocene and Pliocene basalts described by Bonham in northwestern Nevada are directly correlative with age-dated basalts in Oregon. These basalts are late Miocene (14.5 m.y.) in age. In northwestern Nevada, the basalts are intercalated with Pliocene age rocks and overlie "well-dated Miocene rocks at many ... localities" (Bonham, 1969). In the west-central Smoke Creek Desert, and elsewhere in northwestern Nevada, the basalts predate late Pliocene Basin and Range faulting. These stratigraphic relationships bracket its age between late Miocene and late Pliocene. More precise age dating is not possible at present.

Pre-Lake Lahonton Sediments (Qtg)

Pre-Lake Lahonton sediments in the west-central Smoke
Creek Desert are the dissected and faulted remnants of co-
alesced alluvial fans and colluvium. The maximum exposed
thickness of the sediments is about 300 feet (91 m). The
sediments unconformably overlie eroded and faulted upper
Miocene and Pliocene basalts (Tba), and are unconformably
overlain by Pleistocene Lake Lahonton deposits.

Lithology: The clastic material in fans and colluvium
is derived from the basalts. The sediments in the fans are
thinly-to-thickly bedded, poorly consolidated sands and
gravels, with minor intercalated layers of poorly consoli-
dated tuffaceous sedimentary rocks.

Age: These sediments were deposited after late Pliocene
or early Pleistocene normal faulting affected the basalts,
and before late Pleistocene Lake Lahonton occupied the Smoke
Creek Desert basin.

Lahonton and Post-Lahonton Lake Deposits (Qlh)

Deposits of two lacustral intervals defined by Morrison
and Frye (1965), the upper Pleistocene to Holocene Sehoo
Formation and the Holocene Fallon Formation, probably are
present at the surface in the west-central Smoke Creek Desert.
Lake deposits of the Sehoo Formation, defined by Morrison and
Frye (1965, p. 15) as "late Lake Lahonton" in age, are found
below an elevation of approximately 4,370 feet (1332 m) within

the Lahonton Basin. Lake deposits of the Fallon Formation,
defined by Morrison and Frye (1965, p. 19) as "post-Lake
Lahonton" and Holocene in age, are found below approximately
3950 feet (1204 m) in the Pyramid Lake basin (Morrison and
Frye, 1965), and below approximately 3915 feet (1190 m) in
the Black Rock Desert (J.O. Davis, personal communication,
1978). I have classified lake deposits within the Smoke Creek
Desert as "Sehoo" and "Fallon" on the basis of elevation, de-
fining those above approximately 3950 feet (1204 m) as Sehoo
(Lahonton) deposits and those below approximately 3950 feet
(1204 m) as Fallon (post-Lahonton) deposits. This suggested
division is not based on field evidence from within the Smoke
Creek Desert basin. The approximate high shoreline of Holocene
Fallon Lake (from Morrison and Frye, 1965) is shown on Plate 1.

Lithology: The deposits are primarily beach and shallow-
lake sands and silts. Coarse gravel interbedded with sand
is exposed 10 feet (3 m) below the surface in a small quarry
(see Plate 1, the southern end of fault B). Silts and clays
of deeper-lake origin are mostly buried, but pits dug into
the Holocene Playa (2.5 feet or 0.8 m deep) revealed clays
containing ostracods at a depth of 6 inches (15 cm).

Other fossils, found in Fallon Formation beach deposits,
include egg shells, snail shells, fish vertebrae, and duck
and mammal bones (figs. 8 and 9). Tufa deposits, primarily
of algal origin (Morrison and Frye, 1965), are common in
the Sehoo Formation. These are shallow-water deposits and

Figure 8. Fossiliferous beach sands in the Holocene
Fallon Formation. This outcrop is marked "Fossils"
in the southeast edge of Plate 1 (in pocket). Articu-
lated pelecypod shell in center.
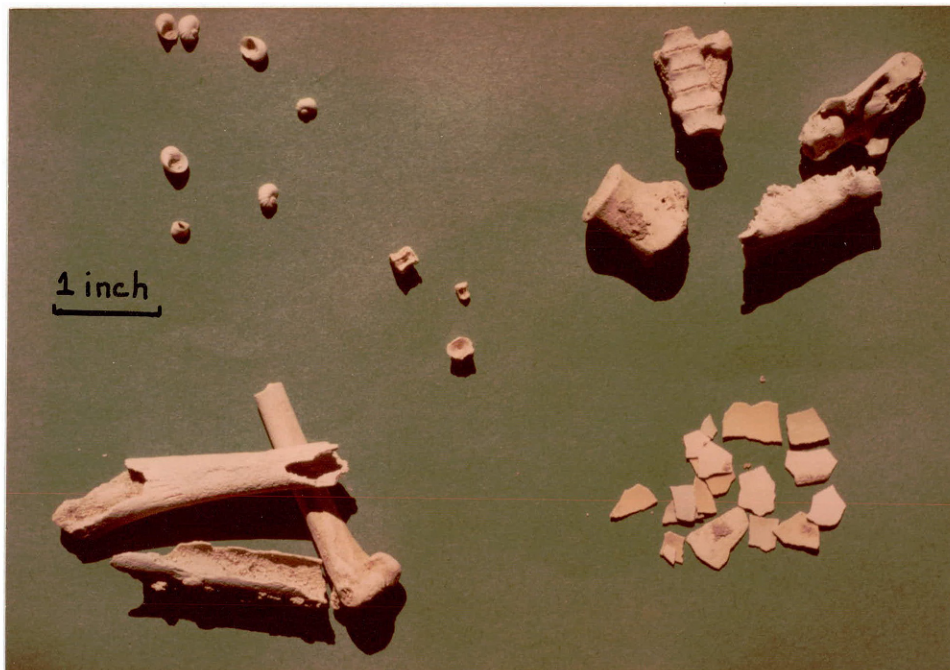
Figure 9. Fossils from the Holocene Fallon Formation
including snail shells, fish vertebrae, egg shells,
duck bones, and mammal vertebrae.

tend to parallel the paleoshoreline. Large reef-like struc-
tures are sometimes present (fig. 10). Several of these
reefs are marked on Plate 1.

Correlation and Age: The suggested correlation of lake
deposits in the Smoke Creek Desert, based on elevation, with
lake deposits of Sehoo and Fallon age within the Lahonton Basin
was discussed on page 21. The Sehoo Formation was deposited
between 25,000 and 7,000 (?) years ago, according to radiocar-
bon dates on tufa, gastropod shells, wood, and other organic
debris (Morrison and Frye, 1965). Stratigraphic, radiocarbon,
and climatic data were used to correlate the Sehoo Formation
with the Bonneville Formation of Utah, the deposits of Pine-
dale glaciation in the Rocky Mountains, and a variety of "physi-
cal stratigraphic units" (Morrison and Frye, 1965) including
soils, alluvium, and sand in the southern Great Plains and
eastern Midwest (Morrison and Frye, 1965). Morrison and Frye
(1965) estimate the time of deposition of the Fallon Formation
as within the last 4000 years. The first lake maximum occurred
about 3,500 years ago and the last about 100 years ago.

Post-Lake Lahonton Sediments (Hal)

Post-Lake Lahonton sediments consist of alluvial material
in fans, intermittent streams and delta-like platforms built
on the Holocene playa, and minor eolian deposits (designated
by "dunes" on Plate 1). Alluvial fans are composed predomi-
nantly of sands and gravels derived from the Mio-Pliocene

Figure 10. Reef-like tufa deposits in the
Pleistocene Sehoo Formation.

basalts (Tba) and tuffaceous sedimentary rocks of the High

Rock sequence (Tts). The sediments overlie older deposits

unconformably. Sediments of intermittent streams are depos-

ited in channels excavated into the older deposits. They

consist of sand- and silt-sized detrital material derived

from the basalts and tuffaceous sediments, and of reworked

lake sediments. The delta-like deposits form elevated lobate

platforms about 3 feet (1 m) high on the surface of the Holo-

cene playa. The deposits are fine sand and silt and form

where intermittent streams empty onto the flat playa surface.

Eolian deposits are not widespread. They form dunes up to

30 feet (10 m) high, which are stabilized by vegetation.

These deposits are Holocene and are time-equivalent in part

with Holocene deposits included in the Lahonton and post-

Lahonton lake deposits (Qlh).

Holocene Playa Surface (Hpl)

The Holocene playa is a flat, barren deflation surface,

which is periodically flooded after heavy rains. During the

early 1950's a small lake occupied the western part of the

playa, below 3845 feet (1192 m) in elevation. Today driftwood

marks the former shoreline of this lake (fig. 11).

Deflation has eroded approximately 30 feet (9.3 m) of

upper Pleistocene and Holocene lake deposits from the central

part of the Smoke Creek Desert basin. According to Sinclair

(1963) deflation has proceeded nearly to the water table on

Figure 11. Driftwood marks the former shoreline of a
small lake. View towards the northwest.

Figure 12. "Rolling boulder" on the Holocene Playa
surface. View towards the west.

the surface of the playa. The water table is less than ten
feet below the surface, and the capillary fringe intersects
the ground surface (Sinclair, 1963).

Saline ground water discharging at the surface by evapor-
ation leaves evaporite minerals in the surficial sediment.
The resulting surface has a puffy, porous texture known as
"puffy ground" (Neal and Motts, 1967). Most of the Holocene
Playa surface has this texture (see fig. 12, p. 27). Where
water has flowed across the playa surface, as after a heavy
rainfall, the surface is washed clean of salts and a hard,
mud-cracked surface develops. The puffy ground surface layer
is 1 to 3 inches thick (2.5-7.5 cm), and the mud-cracked sur-
face layer is about 1 inch thick (2.5 cm). Figure 13 is an
aerial view of the Holocene Playa surface, showing both the
puffy ground (light gray) and the mud-cracked ground (dark
gray). Beneath the surface layer the playa is floored by
lacustral muds (fig. 14).

Figure 12 (p. 27) also shows a "rolling boulder" similar
to those described in Death Valley by Sharp and Carey (1976).
The boulder is moving eastward across the nearly flat playa
surface, apparently moved by the wind when the playa surface
is wet (Sharp and Carey, 1976).

STRUCTURAL GEOLOGY

Structural deformation in the west-central Smoke Creek
Desert is limited to high-angle normal faults and associated

Figure 13. Aerial view, looking south, of the Holo-
cene Playa surface (Hpl). The light surface is
"puffy ground", and the dark surface is mud-cracked.
Three hills are erosional remnants of lake deposits (Qlh).
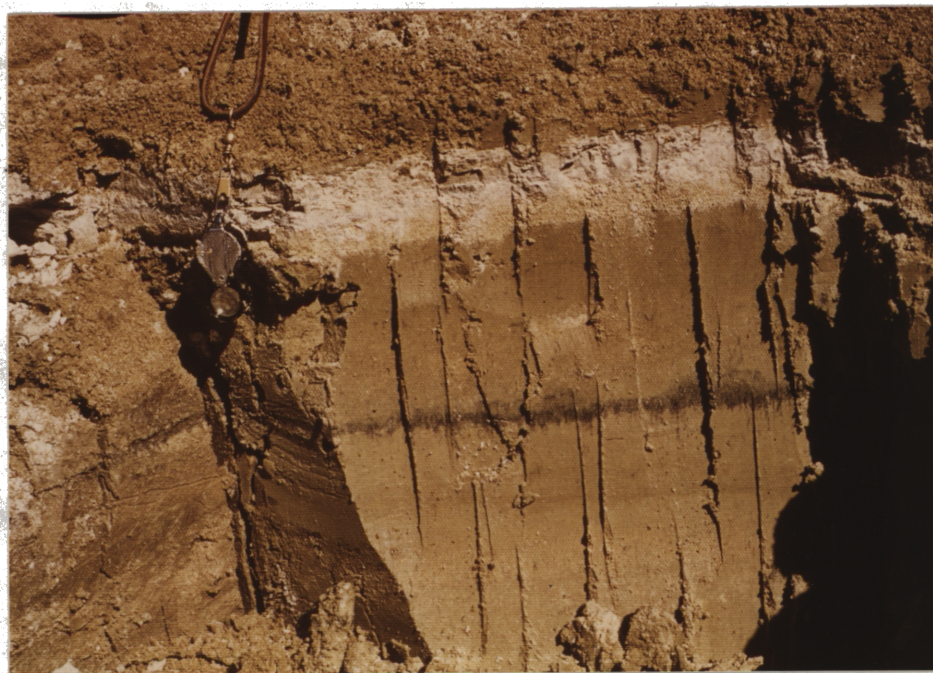
Figure 14. Pit in Holocene Playa surface. White
material is volcanic ash.

gentle tilting. The faults can be separated into two groups
on the basis of age of displacement. Movement occurred along
five faults in the west-central Smoke Creek Desert during the
late Pliocene to early Pleistocene epochs and along eleven
faults during the Holocene Epoch.

Late Pliocene and Early Pleistocene Faults

During the late Pliocene and early Pleistocene volcanic
rocks of the Modoc Plateau were broken into a series of
basins and ranges by a set of predominantly north- to
northwest-trending en-echelon normal faults (Bonham, 1969).
Four faults of this set are present in the west-central Smoke
Creek Desert (faults A, B, C, and D, Plate 1). The downthrown
blocks of these faults are partially or totally buried by
Lake Lahontan sediments that were deposited during the late
Pleistocene Epoch.

The scarps associated with three of these faults (A, B,
and C) define the modern topographic boundary between the
Modoc Plateau and the west-central Smoke Creek Desert. These
three faults extend out of the field area to the north and
south, but are only seven to ten miles (11.3 to 16 km) in
length. The faults trend between $N15^{o}E$ and $N15^{o}W$ and are
downthrown to the east. The maximum westward tilt on the
downthrown blocks is 3° west, assuming that ash-falls in the
basalt (Tba) that now dip $3^{o}W$ were deposited horizontally. The
amount of displacement on the faults is difficult to determine

because the downthrown blocks are largely buried beneath an
unknown thickness of sediments. At the present time the
maximum topographic relief on the linear scarps associated
with faults A and B is approximately 300 feet (92 m). The
scarp associated with fault C is approximately 90 feet (28 m)
high.

The fault scarps have been dissected by stream erosion
and also exhibit wave-cut terraces created by Lake Lahonton
(see Plate 1 for several locations). Although the dip of
the fault plane is probably about 60° (Slemmons, 1957), the
slope of the modern scarps averages only 40°. The tops of
the scarps are rounded, and the bottoms merge into sedimen-
tary cover.

A fourth fault (D, Plate 1) also offset basalts of the
Modoc Plateau during the late Pliocene or early Pleistocene
Epoch. This fault is mostly buried beneath an unknown thick-
ness of upper Pleistocene and Holocene sediments. Only the
edge of the upthrown block is exposed in the field area.
The trend and amount of displacement are uncertain.

A fifth fault of Pleistocene age offsets pre-Lake
Lahonton sediments (Qtg) that were eroded off the upthrown
block of fault B and coalesced into an alluvial apron on
the downthrown block. This fault (E, Plate 1) is pre-Lake
Lahonton (pre-late Pleistocene) in age, as shown by wave-cut
terraces on the scarp associated with the fault. This normal
fault is downthrown to the east and trends $N20^\circ E$. The

downthrown block tilts 3° west, and the scarp face slopes 50° east.

Holocene Faults

Eleven normal faults (F-P, Plate 1) displace shoreline and shallow-water lake deposits of the Holocene Fallon Formation, which have been deposited in the last 4000 years (Morrison and Frye, 1965). The faults trend between $N35^\circ E$ and $N15^\circ W$, range in length from 3300 feet (1007 m) to $3\frac{1}{4}$ miles (6 km), and are all downthrown to the east. The most obvious fault indicators are 1) features associated with ground water blockage along the faults and 2) linear fault scarps.

Ground Water Blockage Along Holocene Faults in the West Central Smoke Creek Desert

Fault gouge zones developed in alluvial materials are reported as barriers to ground water movement by several authors, at several localities in the western United States. The water table is elevated on the up-slope side of the fault; the amount of elevation depends on the hydraulic conductivity of the gouge zone (Williams, 1970). Water movement through the gouge zone is also controlled by this factor.

Basset and Kupfer (1964) reported ground water blockage along the right-lateral Mesquite Lake fault, which cuts alluvium in the Mojave Desert of southern California. Merifield and Lamar (1975a) cite several faults through alluvium and Quaternary lake sediments as barriers to ground water flow

in the Salton Trough area of southern California. Williams
(1970) described elevated water tables on upthrown blocks
of alluvium along normal faults in the Owens Valley of Cali-
fornia. Huntley (1976) described a similar phenomenon along
normal faults in the San Luis Valley of Colorado. Merifield
and Lamar (1975b) catalogued several features associated with
ground water blockage along faults, particularly "spring
alignments, and linear differences in vegetation or land use
along or on opposite sides of a fault". These features are
evident, and in some cases prominent, along faults in Holo-
cene lake deposits in the west-central Smoke Creek Desert.

Alignments of springs and seeps occur along faults F,
G, and H (Plate 1). The springs form small, shallow ponds
three to ten feet (1-3 m) across and a few inches (5-10 cm)
deep. These ponds are usually choked with dense growths of
reeds. Figure 15 shows one such reed-filled spring (0131,
fault G, southwest portion of Plate 1). Irregularly-spaced
small seeps also are numerous along the three faults.
Figure 16 shows several clumps of reeds localized in small
seeps along fault F. Figure 3 (p. 7) shows a narrow, linear
concentration of trees growing along fault F because of
abundant soil moisture. A linear vegetation anomaly also
follows the trace of fault P, although no springs or seeps
were found.

In addition to linear vegetation anomalies concentrated
directly along the trace of the fault, obvious vegetation

Figure 15. Reeds fill spring 013I on the down-
thrown side of fault G. The wash slope is covered
with short grass. Unvegetated slope in background
is debris slope.

Figure 16. Clumps of reeds mark irregularly-
spaced seeps. Grass covers wash slope; debris slope
is sparsely vegetated. Located on fault F.

differences exist in zones on opposite sides of the faults. Figures 15 and 16 show grass covering the downthrown side of faults F and G, in contrast to the normal sage and rabbit brush on the upthrown side. These grassy zones may be several hundred feet wide and commonly are fenced in and used as select cattle pasture, generally for valuable bulls. Another example of vegetation difference on opposite sides of faults is shown in figure 17. The denser vegetation on the upthrown sides of faults M and N indicates that the water table is shallower there.

Another unusual feature, which is also probably associated with disruption of ground water movement by faulting, is found in the Holocene Playa on the southern end of fault O. The trace of this fault is marked on the surface of the playa by a conspicuous linear feature composed of massive crystalline $CaCO_3$ (tufa) thirty to fifty feet (9-15 m) wide, which extends to an unknown depth. Figures 18 and 19 (p. 37) are aerial and ground views of this feature, respectively. The origin of this feature is uncertain, but I think that fault O displaced a confined aquifer within the basin, and that ground water has moved to the surface along this fault (artesian wells in the northwest section of the area support the existence of a confined aquifer; see Plate 1). A possible model suggests that ground water containing calcium bicarbonate seeped into saline lake water (saturated with $CaCO_3$) along the fault, causing precipitation of $CaCO_3$ at and

Figure 17. Aerial view of faults M and N. Denser vegetation is on upthrown sides of faults.
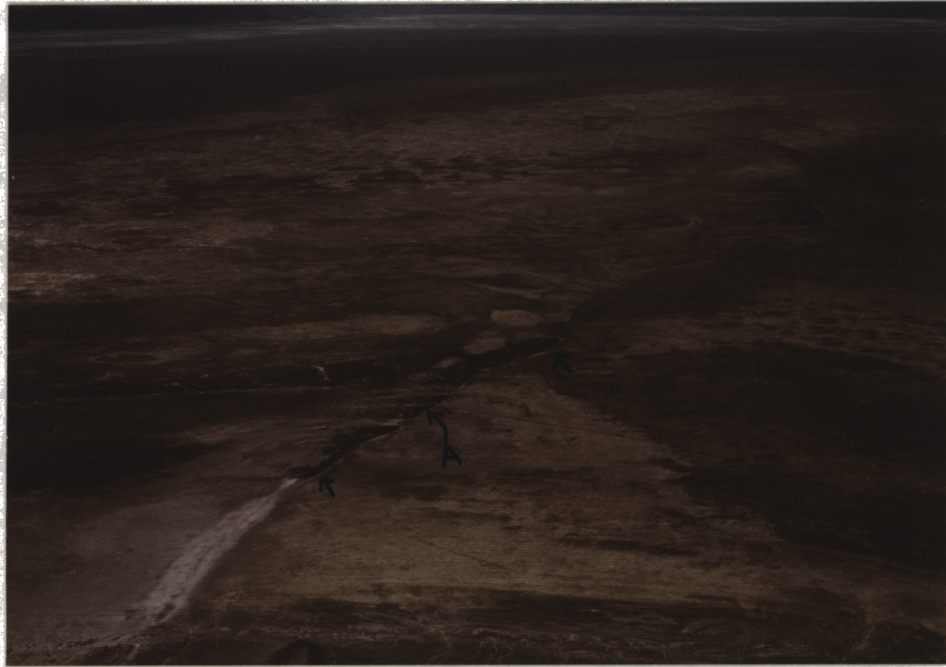
Figure 18. Aerial view, looking south, of the southern end of fault O. Arrows show $CaCO_3$ deposit.

Figure 19. Ground view of $CaCO_3$ deposit, looking north. Located at "A" in figure 18.

near the surface. Sinclair (1963) and Anderson (1975) both
report calcium and bicarbonate in modern Smoke Creek Desert
ground water. This model is based on similar occurrences of
tufa in the Mono Lake basin, California (Dunn, 1953, Lee,
1969, and Keenan Lee, personal communication, 1978).

Not all springs in the study area are fault related. A
few are present where stream erosion (030III, northeast por-
tion of Plate 1) or deflation (020II, central portion of
Plate 1) has intersected the water table. Locations and
temperatures of several springs included in a temperature
survey are shown on Plate 1.

Holocene Fault Scarps in the West-Central Smoke Creek Desert

Linear fault scarps are present along all of the Holo-
cene faults (and most of the Pleistocene faults) in the field
area. The scarps range in height from three feet to eighteen
feet (1 m to 5.5 m). Figure 20 shows the geomorphic charac-
teristics of young fault scarps in alluvial material, as
described by Wallace (1977) in north-central Nevada. The "wash
slope" and the "debris slope" predominate on scarps in the
west-central Smoke Creek Desert (a "free face...the exposed
surface resulting from faulting or succeeding gravity spal-
ling" is not preserved on any of the scarps in the study
area). The debris slope is the "talus slope accumulated
below the free face", and the wash slope is "any part of the
scarp controlled by fluvial erosion or deposition."
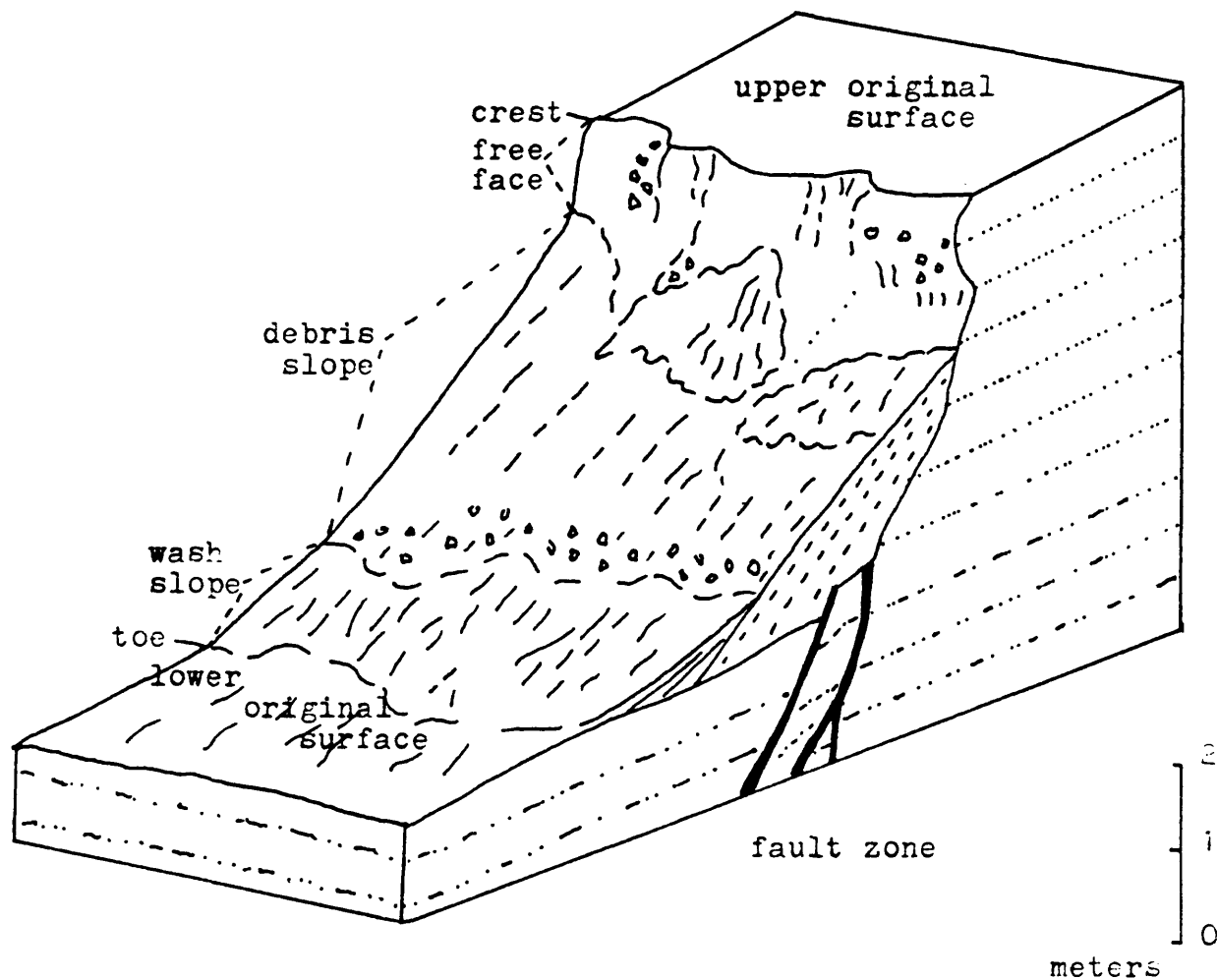
Figure 20. Geomorphic characteristics of young
fault scarps (after Wallace, 1977)

The scarps that have developed along faults with springs and seeps differ slightly from those with no springs and seeps. In both cases the crests of the scarps are rounded and the debris slope dips between 30° and 35°. Along faults with springs and seeps, the wash slope is built up because vegetation on the downthrown side of the fault traps material washed off the debris slope. This accumulation may extend out forty feet (12 m) beyond the base of the debris slope, but is usually less than twenty feet (6 m) wide. The wash slope on the faults without springs and seeps is usually less than five feet (1.5 m) wide. Figure 16 (p. 34) shows the scarp associated with fault F, directly west of the spring designated S22Ib on Plate 1. The partially vegetated slope behind the spring is the debris slope. The wash slope extends to the bottom of the picture and is covered with grass. Figure 15 (p. 34) shows the scarp associated with fault G, at the spring designated 013I. Again the debris slope is covered with grass. Figure 17 (p. 36) is an aerial view of the scarps associated with faults M and N (see Plate 1).

Several of the scarps have been partially eroded away by alluvial and eolian processes. The Smoke Creek and several tributaries have dissected scarps F, K, L, and M and eroded away the southern end of scarp G and the northern end of scarp F. The southern third of scarp O has been removed by a combination of deflation and water erosion (the trace is marked by the $CaCO_3$ discussed earlier).

Repeated movements along faults in the west-central
Smoke Creek Desert

The scarp along fault F increases gradually from about
four feet (1.2 m) high at its southern end to over eighteen
feet (5.4 m) high at its northern end. The northern eight
hundred feet (244 m) has a step-like configuration, which
may have resulted from repeated movement along the fault
(Wallace, 1977). Because the northern end of the fault has
been eroded away to an uncertain extent, interpretation is
difficult, but the unusual height and step-like configuration
of the scarp suggest repeated movement.

Holocene movement on fault O was preceded by early or
middle Pleistocene movement on fault D. Because the exact
trend of fault D is obscured by lake deposits, there is a
possibility that faults D and O are coincident in location.
If this is the case, repeated movement has occurred on the
fault. Figure 21 shows the central and northern trace of
faults O and D. Figure 18 (p. 37) shows the southern trace
of fault O.

RELATION OF THE WEST-CENTRAL SMOKE CREEK DESERT STRUCTURE
TO REGIONAL TECTONICS

The west-central Smoke Creek Desert is in the north-
western Great Basin section of the Basin and Range Province
(fig. 22). The Basin and Range is widely recognized as a
system of horsts and grabens produced by deep crustal and
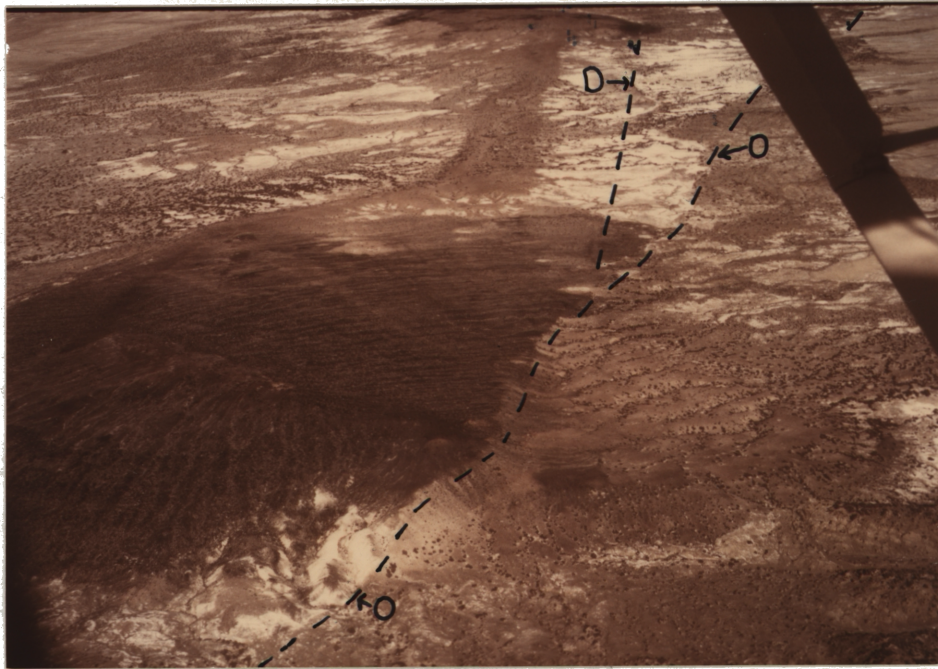
Figure 21. Aerial view, looking north, of the
central and northern trace of fault O, and the
approximate location of fault D.
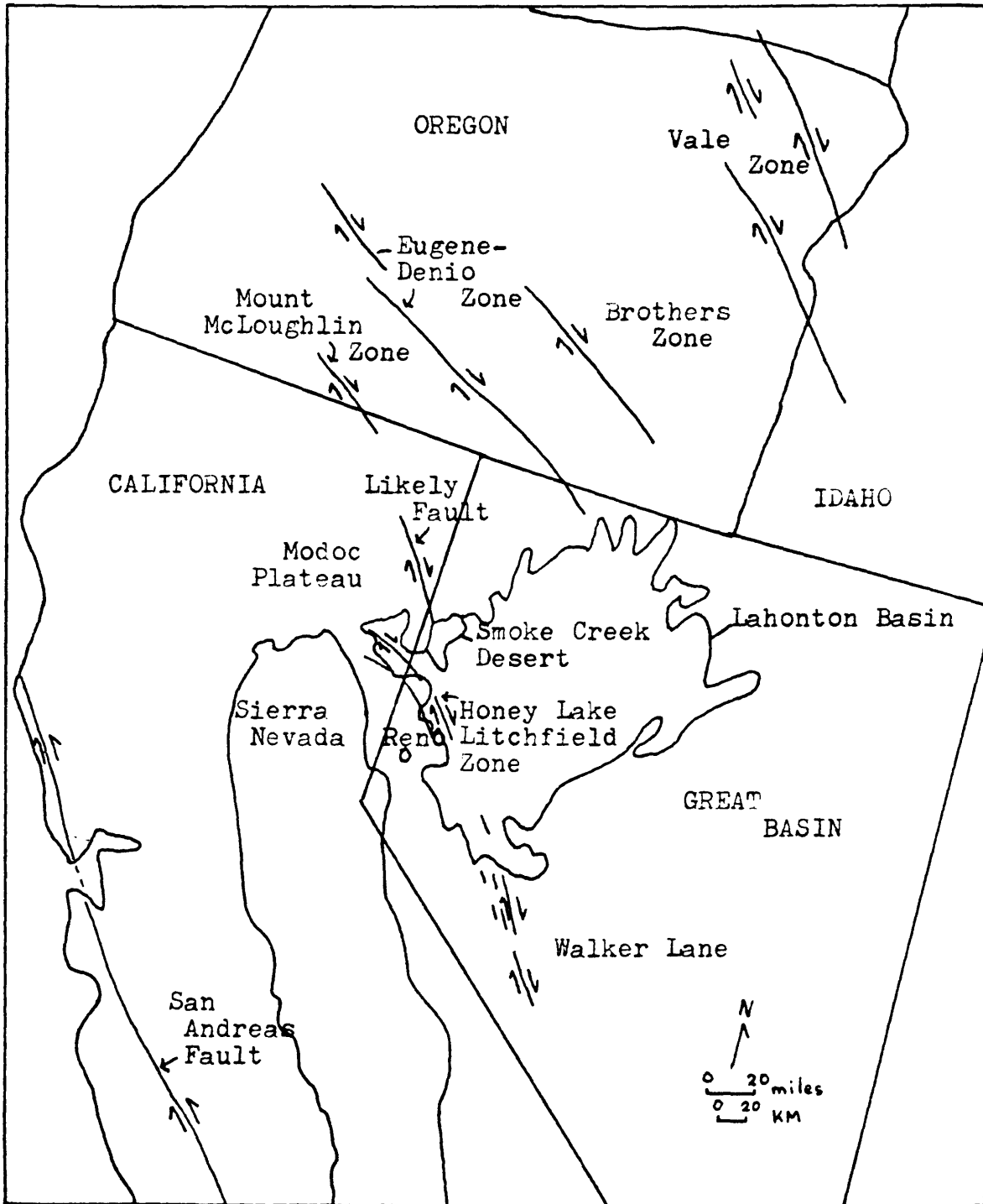
Figure 22. Regional map of western United States, showing major strike-slip fault zones (after Wright, 1976).

sub-crustal extension (Stewert, 1971). Scholz and others

(1971) hypothesized that partial melting of the subducted

Farallon plate produced a diapir in the mantle, which

spread out beneath the crust of the Basin and Range. Figure

23 shows the evolution of Basin and Range structure accord-

ing to this model.

The development of the Great Basin, also according to

Scholz and others' model, is illustrated in figure 24.

While subduction maintained compressive stress towards the east,

large-scale crustal extension was not possible east of the

west coast trench. Release of compressive stress along the

San Andreas transform fault allowed accelerated extension

in the area east of the San Andreas fault, producing the

"bulge" shown in figure 24. This "bulge" area is the modern

Great Basin. More recent studies show that this "bulge" is

defined on the south by the left-lateral Garlock fault

(Davis and Burchfield, 1973), and on the north by a series

of right-lateral faults in northern California and Oregon

(Lawrence, 1976; Wright, 1976).

Lawrence studied four right-lateral, strike-slip fault

zones in northern California and Oregon: the Brothers,

Eugene-Denio, Vale, and Mount McLoughlin zones (fig. 22,

p. 43). Right-lateral offset has resulted from a northward

decrease in east-west extension in the Basin and Range

Province. In areas between the strike-slip zones, Basin

and Range-type normal faulting predominates. Wright (1976)
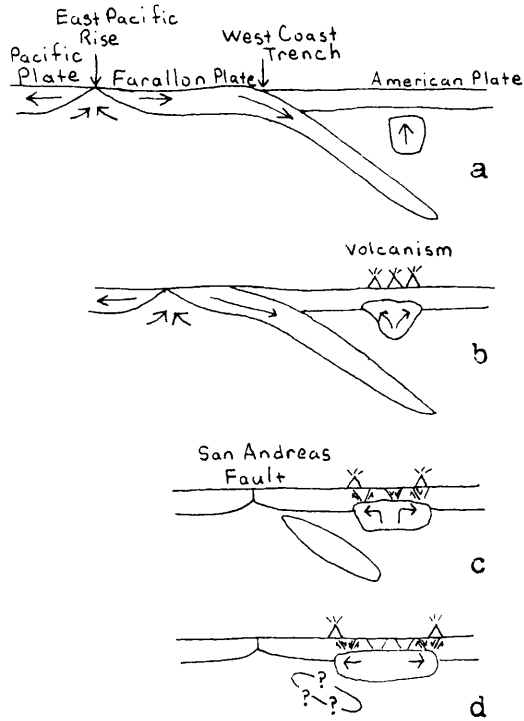
Figure 23. Schematic section across central Nevada showing, from a to d, the inferred Cenozoic evolution of the present Basin and Range structure (after Scholz and others, 1971).

Figure 24. Schematic diagram of the effect of termination of the subduction zone on the west coast on Basin-Range evolution. In a, the heavy line to the left represents the trench off North America, the arrows indicate compressive stresses applied to that boundary. A zone of mantle diapirism is indicated by the stippled region. This zone extended from Canada south to Mexico. In b, the part of the subduction zone opposite Nevada has been terminated, allowing accelerated extension to occur in the Great Basin (after Scholz and others, 1971).
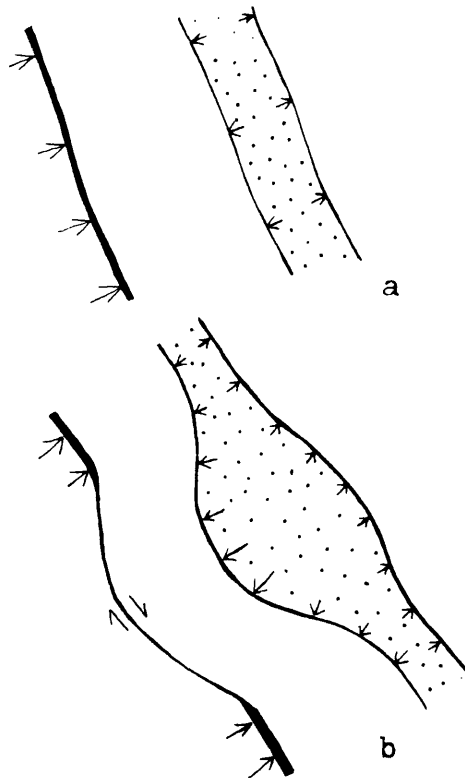
suggests that the right-lateral Likely fault (fig. 22, p. 43) is a member of the set identified by Lawrence.

Wright has defined two separate deformational fields within the Great Basin itself. South of the Walker Lane and Honey Lake-Litchfield right-lateral fault zone (fig. 22, p. 43), gently-dipping normal faults coexist with complementary right- and left-lateral faults. North of the right-lateral zones, extension decreases and steeply-dipping normal faults predominate.

The west-central Smoke Creek Desert is in the steeply-dipping normal fault zone described by Wright (1976). It also lies in an area between two northwest-trending right-lateral features, the Likely fault to the north and the Honey Lake-Litchfield zone to the south (fig. 22, p. 43). In the area between the two right-slip fault zones, which includes the central and southern Smoke Creek Desert basin and the Pyramid Lake basin, normal faults predominate (fig. 25). Figure 25 is a map showing historic seismicity in the Smoke Creek Desert and surrounding areas. Seismic activity appears to be concentrated along the trends of the right-slip fault zones. Between the two, seismicity is of lesser magnitude and intensity.

In spite of the seismicity along the trend of the Likely fault, no surface displacement of strike-slip nature is apparent in the west-central Smoke Creek Desert. At least three separate periods of normal faulting are evident in the
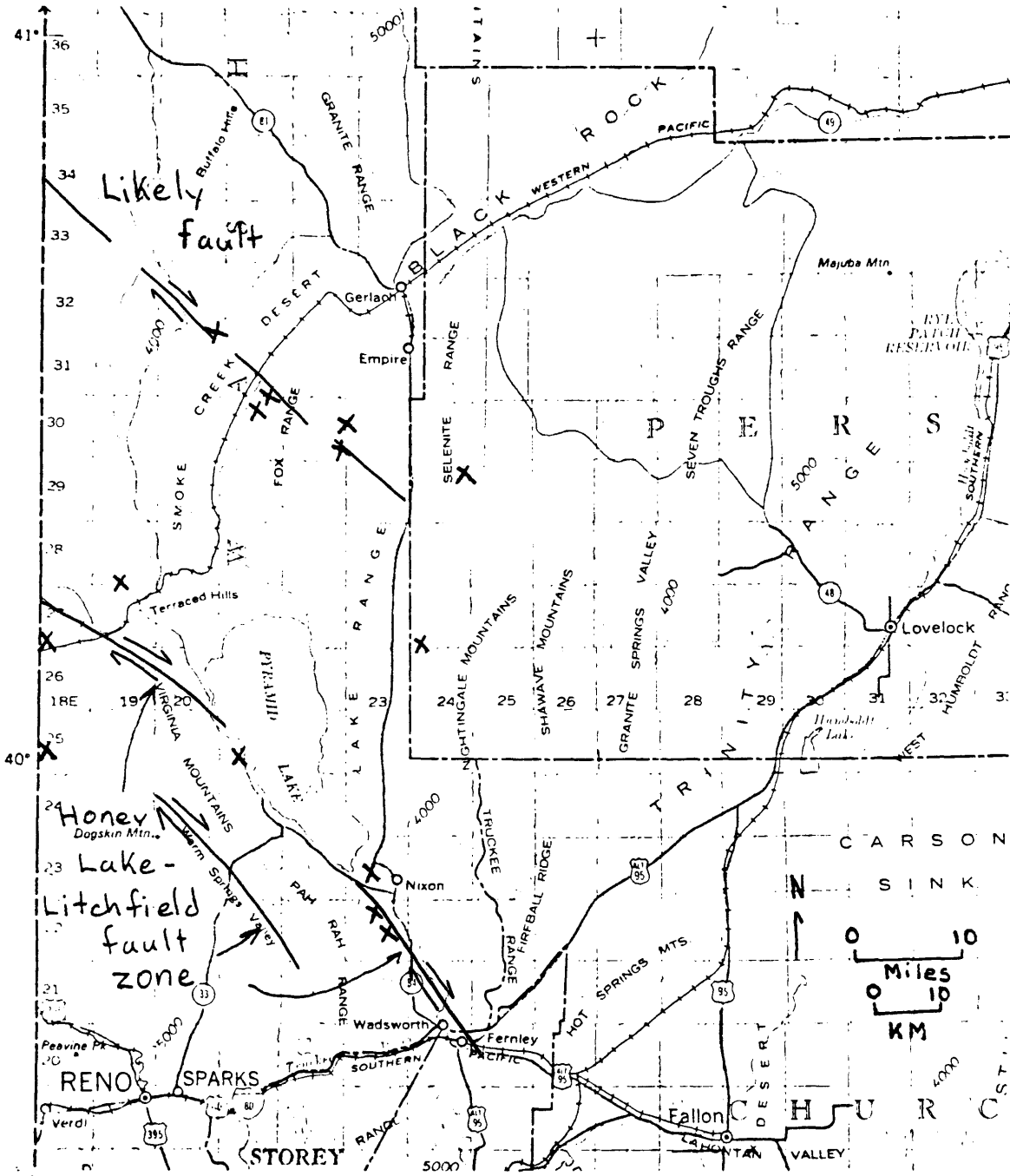
Figure 25. Approximate locations of historic earthquakes
of magnitude between 4 and 6 in the northwest Nevada region
(from Nevada Seismological Laboratory bulletins).

west-central Smoke Creek Desert. Movement occurred along
faults A through D during late Pliocene or early Pleistocene
time (p. 30). Later movement occurred on fault E, before
late Pleistocene time, and faults F through P moved during
the Holocene epoch (p. 32). Deep-crustal and sub-crustal
extension has probably been continuous, but based on mapping
in the west-central Smoke Creek Desert, normal faulting
in the crustal block between the Likely fault and the Honey
Lake-Litchfield fault zone has been periodic in nature.

Differential extension between the normally-faulted
block containing the west-central Smoke Creek Desert and
blocks to the north and south is accomodated along the
strike-slip faults. It is hypothesized that strike-slip
faulting is also periodic in nature, alternating with normal
faulting. Modern seismicity seems to be concentrated along
the strike-slip faults. Accurate age dating of fault movements
would be required to test this hypothesis.

EVALUATION OF SKYLAB PHOTOGRAPHS

INTRODUCTION

The major purpose of this research was to evaluate
Skylab photographs for mapping Quaternary geologic features
in the Basin and Range province that might serve as indica-
tors of geothermal activity. Quaternary faulting and spring
activity were chosen as primary indicators. Discrimination
of surface units received secondary emphasis.

Northwestern Nevada was chosen as a test site for
several reasons:

(1)   excellent S190A and S190B photography is available
      for the area,

(2)   several Known Geothermal Resource Areas ("KGRA")
      are in the area covered by Skylab,

(3)   Quaternary faulting is widespread in the
      northwest Nevada region,

(4)   geologic maps at a scale of 1:250,000 are avail-
      able for the area, and

(5)   larger-scale geologic maps of several geothermally
      active areas in the region are available.

The research was carried out in three phases:

Phase 1 involved laboratory analysis of the Skylab
transparencies and proceeded in two steps. A training area
was defined as the central and southern Black Rock Desert.
Photo-interpretation of Skylab S190A and S190B photographs

was carried out and the interpretation was correlated with small- and large-scale geologic maps. This procedure allowed the interpreter to identify and become familiar with the appearance of recent faulting and associated spring activity. Criteria were developed for future photogeologic interpretation of faults and springs. In a second step of Phase 1, study of Skylab photographs was extended to the north and south of the training area and a site was picked for more detailed mapping and field checking. The west-central Smoke Creek Desert was chosen for reasons to be discussed later. Photogeologic interpretations in the field area were recorded, and criteria were developed for discriminating surface units.

Phase 2 encompassed eight weeks of field mapping, using color-infrared photography at a scale of 1:30,000 as a base. An area of approximately 140 square miles (224 sq. km) of the west-central Smoke Creek Desert was mapped in this phase. This approach was taken to provide a 1:24,000 scale geologic map to be used in evaluating the Skylab photogeologic interpretations recorded in Phase 1.

Phase 3 consisted of a detailed comparison of the Skylab photogeologic interpretations of the west-central Smoke Creek Desert with published geologic maps (scale of 1:250,000) and with the field map prepared in Phase 2. Specifically, the ability to discriminate faulting, springs, and surface units through interpretation of Skylab photographs was evaluated. The three phases will be discussed in detail.

DISCUSSION

Phase 1

Laboratory work during Phase 1 involved analysis of Skylab photographic transparencies, using a Bausch and Lomb zoom stereoscope for magnification up to 14X. Four types of film were initially evaluated, S190A color, color infrared, and black and white (red band), and S190B color photography (see pages 6 and 8 for description of Skylab system). Initial evaluation indicated that, for the purpose of this research, the S190A color and black and white photographs contained no uniquely valuable information that could not be obtained by using the S190A color infrared and S190B color photographs in conjunction. Therefore, the evaluation was restricted to S190A color infrared and S190B color photographs. Plates 2 and 3 (in pocket) are reproductions of the S190B and S190A transparencies described on page 8, respectively. Plates 4 and 5 (in pocket), which are annotated with photointerpretation, show the training area and field area, and selected geographic locations.

Photointerpretation over the training area was annotated on acetate overlays, which have been reproduced on Plates 4 and 5. Because geothermal activity in northern Nevada is concentrated along basin margins (Hose and Taylor, 1974), photointerpretation was also concentrated in these areas. Linear features of possible fault origin were interpreted from the S190B color photographs. Plate 4 shows these features

in the training area. Anomalous dark spots and linear zones
were localized along several of the linears. These were
located on the S190A color infrared photographs, and many
were anomalously red in color, suggesting that they were
associated with vegetation. A smaller number of the dark
spots and zones seen on the S190B color photographs appeared
as dark blue on the S190A color infrared photographs. Recall-
ing that most springs in the Black Rock Desert are associa-
ted with anomalously dense vegetation (Grose, personal com-
munication, 1976), and that faults and springs often are
closely related, I concluded that the red and blue anomalies
possibly recorded relatively dense vegetation associated with
springs. Plate 5 shows the location of color anomalies
interpreted in Phase 1.

After photointerpretation was completed, interpretations
were compared with published geologic maps by Bonham (1969),
Tatlock (1969), and Willden (1964), all at scales of 1:250,000.
Also used for comparison were large-scale geologic maps by
Grose (unpublished geologic map of the Black Rock Fault),
and by Anderson and Sperandio (1975, progress geologic maps
of Gerlach and Hualapai Flat geothermal areas, in Grose and
Keller, 1975), at scales of 1:24,000.

The results of this comparison can be briefly summarized
(refer to Plates 2, 3, 4, and 5).

Linears along the western edge of the Black Rock Range
(see Plate 4) correspond in trend and location to branches

of the Black Rock fault (named by L.T. Grose in 1977 in a
proposal to the U.S. Geological Survey). Particularly,
linears L2, L3, and L4 correspond to Holocene faults on the
Black Rock fault system. Linears west of the Trego rail-
road siding correspond to southern segments of the same
fault system. Linears in the Hualapai Flat correspond in
trend and location to Quaternary faults mapped by Sperandio
(Grose and Keller, 1975). L6 is a Quaternary fault asso-
ciated with the Fly Ranch geothermal springs. Linears west
and south of Gerlach correspond to several Quaternary faults
mapped by Anderson (Grose and Keller, 1975). L7 corres-
ponds to faults in alluvial fan material on the edge of
the Granite Range.

Color anomalies (Plate 5) on the western margin of the
Black Rock Range can be correlated with hot springs occurring
along the Black Rock fault. The Double Hot Springs KGRA is
at the northernmost color anomaly. Color anomalies along
the western side of Hualapai Flat correspond to several
warm and hot springs. The largest anomaly is associated
with the Fly Ranch KGRA. Of the two color anomalies on the
eastern edge of Hualapai Flat, the northern one is associated
with a warm spring (Sperandio, personal communication, 1976),
and the southern is unidentified. Color anomalies near
Gerlach mark the Gerlach Hot Springs (Great Boiling Hot
Springs) on the east and Mud Springs on the west. These two
springs form the Gerlach KGRA. The color anomaly near Trego

is associated with Coyote Spring, a warm spring.

During correlation of linears and color anomalies, criteria were developed for interpreting linears as possible faults and color anomalies as possible spring-related features. Table 1 lists criteria for interpreting Type A linears (probable faults). Table 2 lists criteria for interpreting Type A color anomalies (anomalous zones thought to indicate vegetation associated with springs). These criteria were used in further photointerpretation.

In the second part of Phase 1 photointerpretation of Skylab photographs was extended to the north and south, in order to select an area in which to field check the criteria established in the first part of Phase 1. The west-central Smoke Creek Desert was chosen for several reasons, including the reported existence of two warm springs (Waring, 1965) and the relatively easy access to the area. Additionally, photo-interpretation revealed many linear features that fit the criteria in Table 1, and several color anomalies that fit the criteria in Table 2. Also, in contrast to the training area, several distinctive surface units could be separated in the area. Table 3 (p. 56) shows the characteristics used to define surface units in the west-central Smoke Creek Desert.

Photointerpreted Type A linears, Type A color anomalies, and surface units were annotated on overlays. Plate 6 (in pocket) is an enlarged S190B color photograph, at a scale of

Table 1. Criteria for designating linear features on

Skylab S190B photographs as Type A linears

(probable faults).

1. Obvious topographic relief along a linear

feature, suggestive of a scarp.

2. Obvious color and/or textural differences in

surface material on opposite sides of a linear

feature.

3. Linear features connecting anomalously colored

spots or zones.

Table 2. Criteria for designating anomalously-colored

spots or zones as Type A color anomalies

(probably vegetation associated with springs).

1. Red color on S190A color infrared photographs.

2. Location along a probable fault.

3. Blue anomalies on S190A color infrared photographs

associated with red anomalies.

4. Non-rectangular pattern (such as those associated

with cultivation).

Table 3. Characteristics used to define surface units on S190B color photographs.

Distinguishing characteristics

Unit Name (Plate 8)	Color	Texture	Topographic Relief	Other
A	dark reddish brown	fine grained	moderately hilly topography* cliff-like relief at edges.	
B	gray to pink-* brown	fine grained	moderate rolling relief.	
Qs	light yellow-brown	variable, pock-marked and ridged*	moderate within unit and between this and other units	shoreline traces
Qal	dark brown*	fine grained	none within unit	drainage* pattern
Qp	light yellow	fine grained	none within unit	

* means most distinguishing characteristic

approximately 1:100,000, showing the west-central Smoke
Creek Desert area of study. Plate 7 (in pocket) shows the
Type A linears interpreted from Skylab (nos. 1-24). Plate
8 (in pocket) shows the Type A color anomalies (nos. 1-12)
and the surface units interpreted (the color anomalies are
shown on the S190B because the S190A is very poor in quality
when enlarged to 1:100,000). Plate 7 also shows several
miscellaneous features observed during photointerpretation
that needed to be field checked. This set of features in-
cludes linear features that disrupted alluvial fan deposi-
tion (A), an arcuate zone of red on the S190A photographs (B),
several dark lineations in the area defined as playa (C1-C4),
and a dark arcuate zone in the playa (D).

Phase 2

Because of the variety of features discriminable on the
Skylab photography, and the size of the area to be evaluated,
it was decided that detailed field-checking of specific fea-
tures would be nearly as time-consuming as making a large-
scale geologic map from field work alone. Also, pertinent
geologic information might be overlooked in a field-checking
situation, and a more detailed, large-scale field map would
provide a better basis for evaluating the Skylab photographs.
The objective of field mapping was to identify geologic
features for later correlation with features interpreted on
the Skylab photographs.

Plate 1 (in pocket) is the geologic map developed during

two months of field work during Phase 2. Geologic observations were annotated on 1:30,000 scale color infrared photographs and transferred onto 1:24,000 scale orthophotoquads (large-scale topographic maps were not available during field work). The 140-square-mile (224 sq. km) area was covered by numerous east-west traverses on foot. Observations from two aircraft overflights, one before field work began and one at its conclusion, also aided in mapping.

During field mapping, several faults not previously mapped by other authors were identified (faults A, D, E, I, J, L, M, N, and P, Plate 1), and several new surface units were separated (the breccia pipe and tuffaceous sediment units of the Mio-Pliocene basalts, and the Holocene Playa Surface).

A temperature survey of several springs in the west-central Smoke Creek Desert revealed that nóne is warm according to Nevada Bureau of Mines and Geology standards (greater than $20^{\circ}C$ is considered "warm" for a spring in Nevada, J.H. Schilling, 1976, personal communication). All of the springs in the field area are between $14^{\circ}C$ and $20^{\circ}C$.

Phase 3

The field geologic map (Plate 1) compiled on the 1:24,000 scale orthophotoquads was compared with the Type A linears (probable faults), Type A color anomalies (probable spring-associated vegetation), surface units, and miscellaneous features interpreted from the S190A and S190B photographs (see Plates 6, 7, and 8). The objective of this correlation

was to check the accuracy of the photointerpretation when compared to the actual occurrence of springs, faults, and surface units. Other objectives were evaluation of the resolution of the photographs and determination of scale limitations on geologic mapping.

Plate 7 shows the twenty-four Type A linears interpreted during Phase 1. Sixteen of these linears correspond along all or part of their length with faults mapped in the field, eight of which (linears 1, 3, 8, 10, 11, 14, 15, and 20) are associated with faults not identified by previous authors. Linear 9 is associated with an alignment of two sand dunes, and may mark a buried fault. Sand dune alignments along fault zones, where abundant water supply traps sand, are seen along other fault zones in northwestern Nevada including the Black Rock fault. Linear 24 is drawn through a series of dark lineations on the S190B photograph. Field checking showed these dark areas to be tufa deposits within Lahonton sediments, near the modern interface between coarse-grained shoreline facies and fine-grained playa muds. I believe the $CaCO_3$ was precipitated in shallow saline lake water by springs that were forced to the surface at the facies change. Although they appear linear on the satellite photographs, field investigation revealed that they are discontinuous and patchy in distribution. Six of the linears are not associated with faults mapped by me. One fault identified in the field (H) was not interpreted on the S190B photographs. Data on

the comparison of photointerpreted faults with actual faults is summarized in Table 4.

Plate 7 also shows several miscellaneous features discriminated in Phase 1. The features marked A are sand bars deposited in Lake Lahonton. The dark, arcuate zone outlined at B is pasture land created by several small wells that are allowed to flow directly onto the ground. C1 and C2 are narrow strips of playa surface that have been washed clean of salts. C3 and C4 are remnants of lake sediments (unit Qlh, Plate 1) that form small hills in the playa. The remnants slope gently onto the playa surface, and the slopes are littered with broken crusts of $CaCO_3$. The crusts may have been deposited during a recent high stand of a saline lake in the Smoke Creek Desert basin. Dunn (1953) describes similar crust on the shoreline of Mono Lake, California, and attributes their formation to mixing of saline lake water and fresh ground water or rainwash. Figures 26 and 27 (p. 62) illustrate one of these slopes, which appears as a dark line on the Skylab photographs. The arcuate zone designated D is also a portion of the playa surface that has been washed clean of salts by water flowing across the playa (see figure 13, p. 29, for an aerial view of this feature).

Plate 8 shows the Type 1 color anomalies interpreted from the S190A photographs. All of these are associated with anomalously dense vegetation, which is associated with relatively abundant water supply. A few small springs (O11I,

Table 4. Type A linears and field identification.

Type A linears   Field Identification
   (Plate 7)

        1   Fault A
        2   Fault B
        3   Fault E
        4   Fault C
        5   Fault K
        6   Northern half is Fault G
        7   Southern half is Fault F
        8   Fault I
        9   Alignment of two sand dunes
       10   Fault J
       11   Southern half is Fault L
       12   Southern end of Fault M
       13   Linear segment of a stream
       14   Northern end of Fault M
       15   Fault N
       16   Linear edge of stream channel
       17   Coincidental alignment of spring
                                and shoreline deposit
       18   Southern half is southern end of
                                Fault O
                             Northern half may correspond to
                                Fault D
       19   Northern end of Fault O
       20   Fault P
     21-24   Linear shoreline deposits

Figure 26. Sloping remnants of lake sediments, covered with $CaCO_3$ crusts (see Plate 1, eastern portion, for location). View towards the east.

Figure 27. Close view of $CaCO_3$ crusts.

012I and 012Ia, northeastern portion of Plate 1), with vege-
tation anomalies less than 15 feet (3 m) wide, were not in-
terpreted on the Skylab photographs. Table 5 sum-
marizes the comparison between Type 1 color anomalies and
springs. Plate 8 also shows the surface units discriminated
on the S190B photographs. When compared to Plate 1, the
unit designated A corresponds to the Mio-Pliocene basalts
(Tba). Qal corresponds to the post-Lake Lahonton sediments
(Hal), and Qs corresponds to the Pleistocene and Holocene
lake deposits (Qlh). Qp corresponds to the Holocene Playa
surface (Hpl), and B corresponds to the High Rock Sequence
(Tts). The Cretaceous intrusion (Kgd) and the Pre-Lahonton
sediments (Qtg) were not discriminated on the Skylab photo-
graphs. The breccia pipe and tuffaceous sediment units
(Tbp and Tbt) of the Mio-Pliocene basalts also were not dis-
criminated.

SUMMARY AND CONCLUSIONS

At a scale of 1:24,000, five of seven major units ex-
posed at the surface on the west-central Smoke Creek Desert
were mapped accurately. The two units not discriminated cover
only a few square miles each in the field area. Sixteen
linears interpreted as probable faults (Type A linears) were
identified in the field as actual faults, eight of which cor-
respond to faults not previously mapped by other authors.
Seven linears interpreted as probable faults are actually

Table 5. Type A color anomalies and field identification.

Type A Color Anomaly (Plate 8)	Field Identification
1	Vegetation around spring located at Fault F
2	Vegetation growing around springs and seeps on Fault F
3, 4, 6	Vegetation growing around wells drilled to create pastures
5	Vegetation in springs and seeps along Fault G
7	Vegetation in a stream channel that has cut down to the water table
8-12	Vegetation in springs created by erosion to the water table

linear topographic features related to lake sedimentation,
and one is related to stream erosion. Only one fault iden-
tified in the field was not discriminated during photoin-
terpretation. Twelve Type A color anomalies were interpreted
from the S190A photographs. All of these correspond to
anomalously dense vegetation associated with abundant water,
but three are man-made features. Three linear color anomalies
(1, 2, 5, Plate 8) marked dense vegetation concentrated along
the traces of Holocene faults.

     Linear topographic relief is not a good guide for
fault identification on Skylab photographs, at least not in
the lake deposits in the west-central Smoke Creek Desert.
This conclusion should apply to such deposits in the whole
Lahonton Basin. The shape of the Smoke Creek Desert deposi-
tional basin is structurally controlled, so it is not sur-
prising that depositional features such as beaches and sand
bars are somewhat linear and generally correspond in trend
to the boundaries of the basin (see Type A linears 16, 17,
19, 21, 22, 23, and 24, Plate 7). Linear differences in
vegetation along or on opposite sides of faults, and dif-
ferences in color and texture of surface materials on oppo-
site sides of faults, are easily discriminable on the
Skylab S190B photographs; these are the best guides to fault
interpretation. The correlation between Type A color anomalies
and vegetation associated with abundant water is excellent,
although distinction between wells and springs is impossible

without field checking the photointerpretation. Color and textural differences visible on the S190B photographs are excellent guides to mapping Quaternary sediments. Topography, along with color and texture, is an excellent guide to mapping bedrock units on the Skylab photographs.

Skylab photographs are a good base for mapping faults and surface units, and a good guide to possible springs in the arid terrain typical of northwest Nevada deserts. Photointerpretation of S190A color infrared and S190B color photographs, accompanied by field checking, offers a rapid method of mapping large areas in regions similar to northwest Nevada. In the west-central Smoke Creek Desert, photointerpretation and field checking would have yielded a geologic map of accuracy comparable to the 1:24,000 scale geologic map prepared during two months of field work in Phase 2, in about one-fourth the time. This represents a significant savings of time, and therefore of money.

REFERENCES CITED

Abdel-Gawad, Monel, and Linda Tubbesing, 1975, Analysis of
    tectonic features in U.S. southwest from Skylab
    photographs: Final Report, Rockwell International
    Science Center, Thousand Oaks, Calif., prepared for
    NASA/Johnson Space Center, Houston, Texas, 78 p.

Anderson, J. P., 1975, Preliminary report of geochemical in-
    vestigations of thermal areas in the Gerlach-Hualapai
    Flat-Black Rock Desert-Smoke Creek Desert area: in
    Colorado School of Mines Nevada Geothermal Study,
    Progress Rept. 4, pp. 80-109.

Bassett, A. M., and D. H. Kupfer, 1964, A geologic reconnais-
    sance in the southeastern Mojave Desert: Calif. Div.
    of Mines and Geology Special Report 83, 43 p.

Bonham, H. F., 1969, Geology and mineral deposits of Washoe
    and Storey counties, Nevada: Nevada Bur. of Mines Bull.
    70, 140 p.

Dunn, J. R., 1953, The origin of the deposits of tufa in Mono
    Lake: Journ. of Sed. Petrology, v. 23, p. 18-23.

Grose, L. T., and G. V. Keller, 1974, Report of progress for
    the period May 1, 1974, to July 31, 1974: Colorado
    School of Mines Geothermal Study, 72 p.

Hose , R. K., and B. E. Taylor, 1974, Geothermal systems of
    northern Nevada: U. S. Geol. Survey Open-file Report
    74-271, 27 p.

Huntley, David, 1976, Ground water recharge to the aquifers
    of northern San Luis Valley, Colorado: a remote sensing
    investigation: Colorado School of Mines Remote Sensing
    Report 76-3, 247 p.

Lamar, D. L., and P. M. Merifield, 1975, Final report: Appli-
    cation of Skylab and ERTS imagery to fault tectonics and
    earthquake hazards of the Peninsular Ranges, southwestern
    California: California Earth Science Corporation, Tech-
    nical Report 75-2, 66 p.

Lawrence, R. D., 1976, Strike-slip faulting terminates Basin
    and Range province in Oregon: Geol. Soc. America Bull.,
    v. 87, p. 846-850.

Lee, Keenan, 1969, Infrared exploration for shoreline springs at Mono Lake, California, test site: Stanford Univ. Remote Sensing Lab., Tech. Rept. 69-7, 196 p.

Lee, Keenan, G. L. Prost, D. H. Knepper, D. L. Sawatzky, D. Huntley, and R. J. Weimer, 1975, Geologic and mineral and water resources investigations in western Colorado, using Skylab EREP data: Final Report: Colorado School of Mines Remote Sensing Report 75-5, 52 p.

Lee, Keenan, and R. J. Weimer, 1975, Geologic interpretation of Skylab photographs: Colorado School of Mines Remote Sensing Report 75-6, 75 p.

MacDonald, G. A., 1966, Geology of the Cascade Range and Modoc Plateau, in Geology of northern California: California Div. of Mines and Geology Bull. 190, p. 65-96.

Merifield, P. M., and D. L. Lamar, 1975a, Faults on Skylab imagery of the Salton Trough area, southern California: California Earth Science Corporation, Technical Report 75-1, 23 p.

_____, 1975b, Active and inactive faults in southern California viewed from Skylab: Proceedings NASA Earth Resources Survey Symposium, 1975.

Morrison, R. B., and J. C. Frye, 1965, Correlation of the middle and late Quaternary successions of the Lake Lahonton, Lake Bonneville, Rocky Mountain (Wasatch Range), southern Great Plains and eastern midwest area: Nevada Bureau of Mines Rept. 9, 45 p.

Neal, J. T., and W. S. Motts, 1967, Recent geomorphic changes in playas of western United States: Jour. Geology, v. 75, p. 511-525.

Nevada Bureau of Mines, 1970-1975, Bulletins of the Seismological Laboratory: Nevada Bureau of Mines, Univ. of Nevada, Reno, Nevada.

Scholz, C. H., M. Barazangi, and M. L. Sbar, 1971, Late Cenozoic evolution of the Great Basin as an ensialic interarc basin: Geol. Soc. America Bull., v. 82, p. 2979-2990.

Sharp, R. P., and D. L. Cary, 1976, Sliding stones, Racetrack Playa, California: Geol. Soc. America Bull., v. 87, p. 1704-1717.

Sinclair, W. C., 1963, Ground-water appraisal of the Black
    Rock Desert area, northwestern Nevada: Nevada Dept. of
    Conserv. and Nat. Resources, Ground-water Resources -
    Reconn. Series Rept. 20, 32 p.

Slemmons, D. B., 1957, Geological effects of the Dixie Valley-
    Fairview Peak, Nevada earthquakes of December 16, 1954:
    Bull. of the Seismological Soc. of America, v. 47, no. 4.

Sperandio, R., 1975, Geological mapping in Hualapai Flat,
    Fly Ranch hot spring area: in Colorado School of Mines
    Nevada Geothermal Study, Progress Rept. 4, pp. 3-14.

Tatlock, D. B., 1969, Preliminary geologic map of Pershing
    County, Nevada: U. S. Geol. Survey Open-File Rept.

University of New Mexico Technology Application Center,
    Skylab 3 Photography Catalog: Univ. New Mexico, Albu-
    querque, New Mexico, pp. 1, 1, 43.

Wallace, R. E., 1977, Profiles and ages of young fault scarps,
    north-central Nevada: Geol.Soc. America Bull., v. 88, p.
    1267-1281.

Waring, G. A., 1965, Thermal springs of the United States
    and other countries of the world - a summary: U. S.
    Geol. Survey Prof. Paper 492, 383 p.

Willden, Ronald, 1964, Geology of Humboldt County, Nevada:
    Nevada Bureau of Mines Bull., v. 59, plate 1, Humboldt
    County Map, 1:250,000.

Williams, D. E., 1970, Use of alluvial faults in the storage
    and retention of ground water: Ground Water, v. 8, no.
    5, p. 25-29.

Wollenberg, H. F., F. Asaro, H. Bowman, T. McEvilly, F. Mor-
    rison, and P. Witherspoon, 1975, Geothermal energy
    resources assessment: Energy and Environment Div.,
    Lawrence Berkely Laboratory, University of Calif., 89 p.

Wright, Lauren, 1976, Late Cenozoic fault patterns and stress
    fields in the Great Basin and western movement of the
    Sierra Nevada Block: Geology, v. 4, p. 489-494.
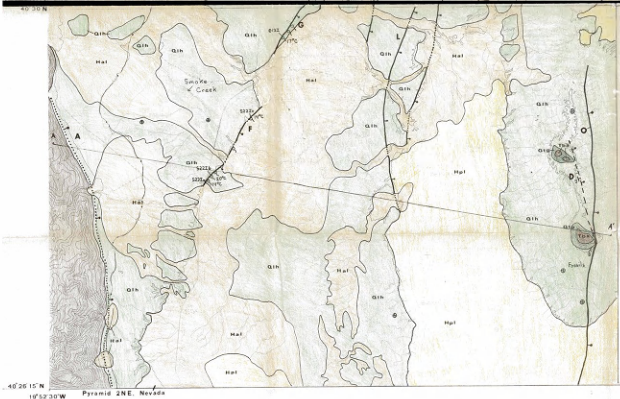
PLATE I

GEOLOGIC MAP
OF THE
WEST-CENTRAL
SMOKE CREEK DESERT
WASHOE COUNTY, NEVADA

by

Rebecca L. Dodge
1978

Scale 1:24,000

true north

magnetic north

Topographic Contour Interval

EXPLANATION

Hpl	Holocene Playa Surface	
Hal	Post-Lake Lahonton Sediment	
Qlh	Lahonton & Post-Lahonton Lake Deposits, Sehoo and Fallon Formations undivided	
Qtg	Pre-Lake Lahonton Sediment	
Tba	Tbt Basalts, Tuffaceous sedimentary rocks Tbp Tbsc, Breccia Pipe (Tbp)	
Tts	High Rock Sequence Tuffaceous Sedimentary Rock	
Kgd	Granodiorite	

Quaternary
Mio-Pliocene
Cretaceous

Fault, ball on downthrown side. Dotted where covered, dashed where inferred

Strike and dip of bedding

Horizontal bedding

Spring, number and temperature

Formation Contact

S   Wave-cut features

CROSS SECTIONS

A — A'

Horizontal Scale 1:24,000
Vertical Exaggeration 2X

B — B'

N

10 miles

326

10 miles

N
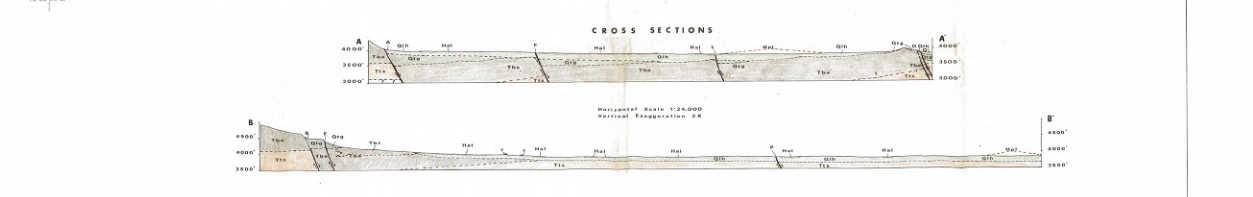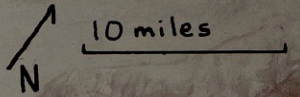
Plate 3. S190A color-infra-
red photograph of north-
western Nevada. Scale approx-
imately 1:950,000.

Plate 4. Possible-fault linears in the training area.

Plate 5. Possible spring-related-vegetation color anomalies in the training area.

Labels visible on the image: Field Area, Smoke Creek Desert, Hualapai Flat, Double Hot Spring, Black Rock Range, Black Rock Desert, Gerlach, Trego, Training Area, Pyramid Lake, N
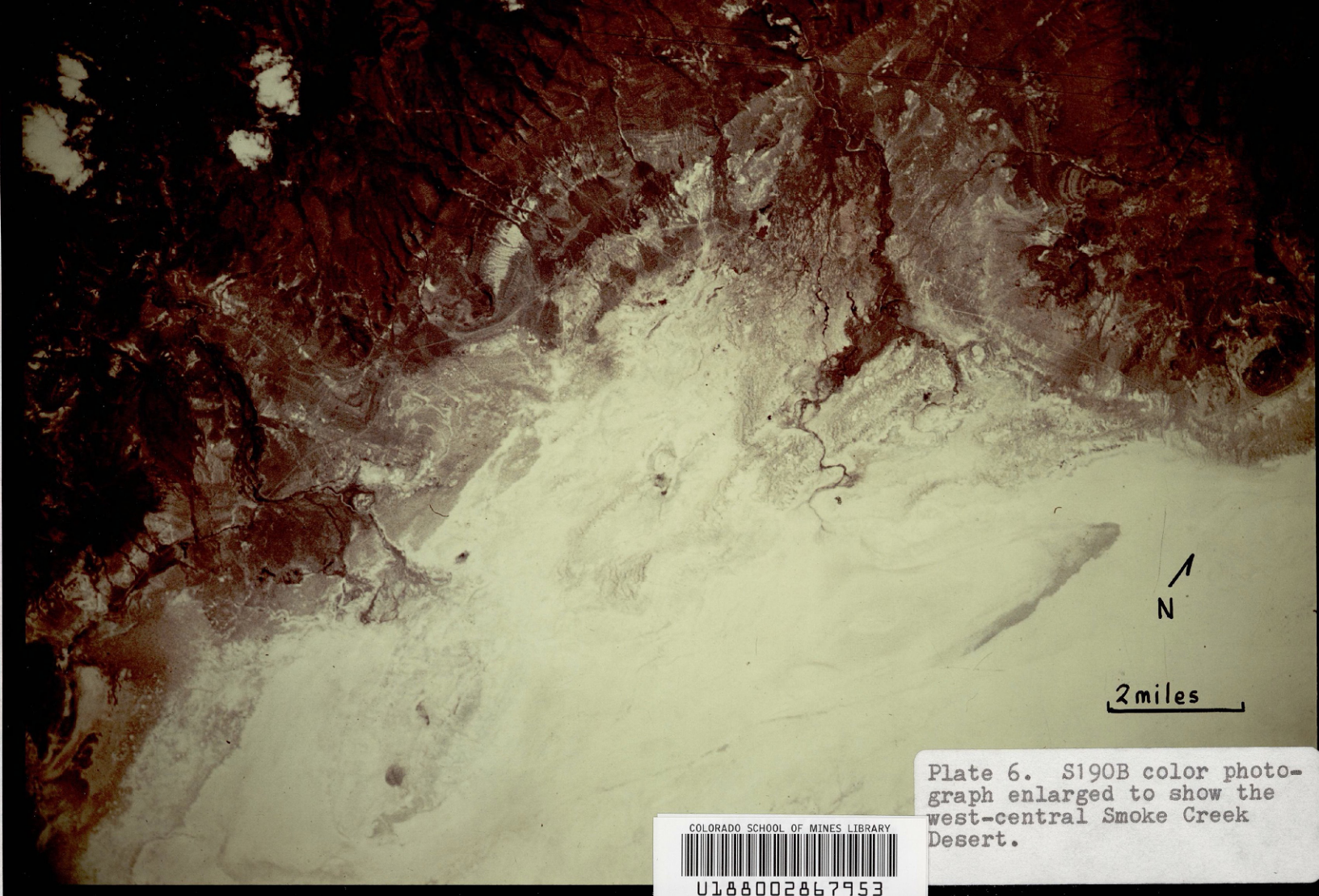
N

2 miles

Plate 6. S190B color photo-
graph enlarged to show the
west-central Smoke Creek
Desert.
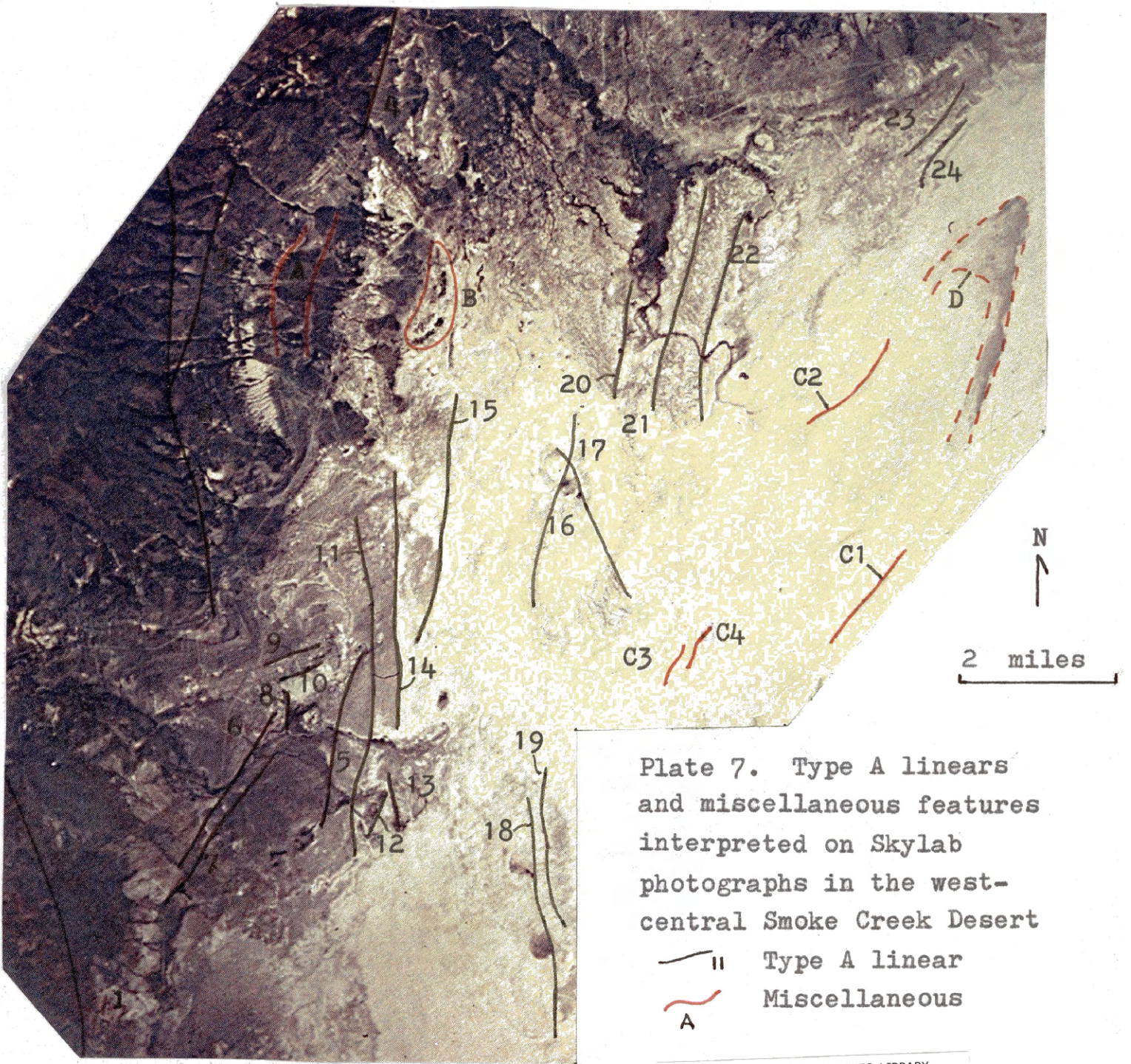
Plate 7. Type A linears and miscellaneous features interpreted on Skylab photographs in the west-central Smoke Creek Desert
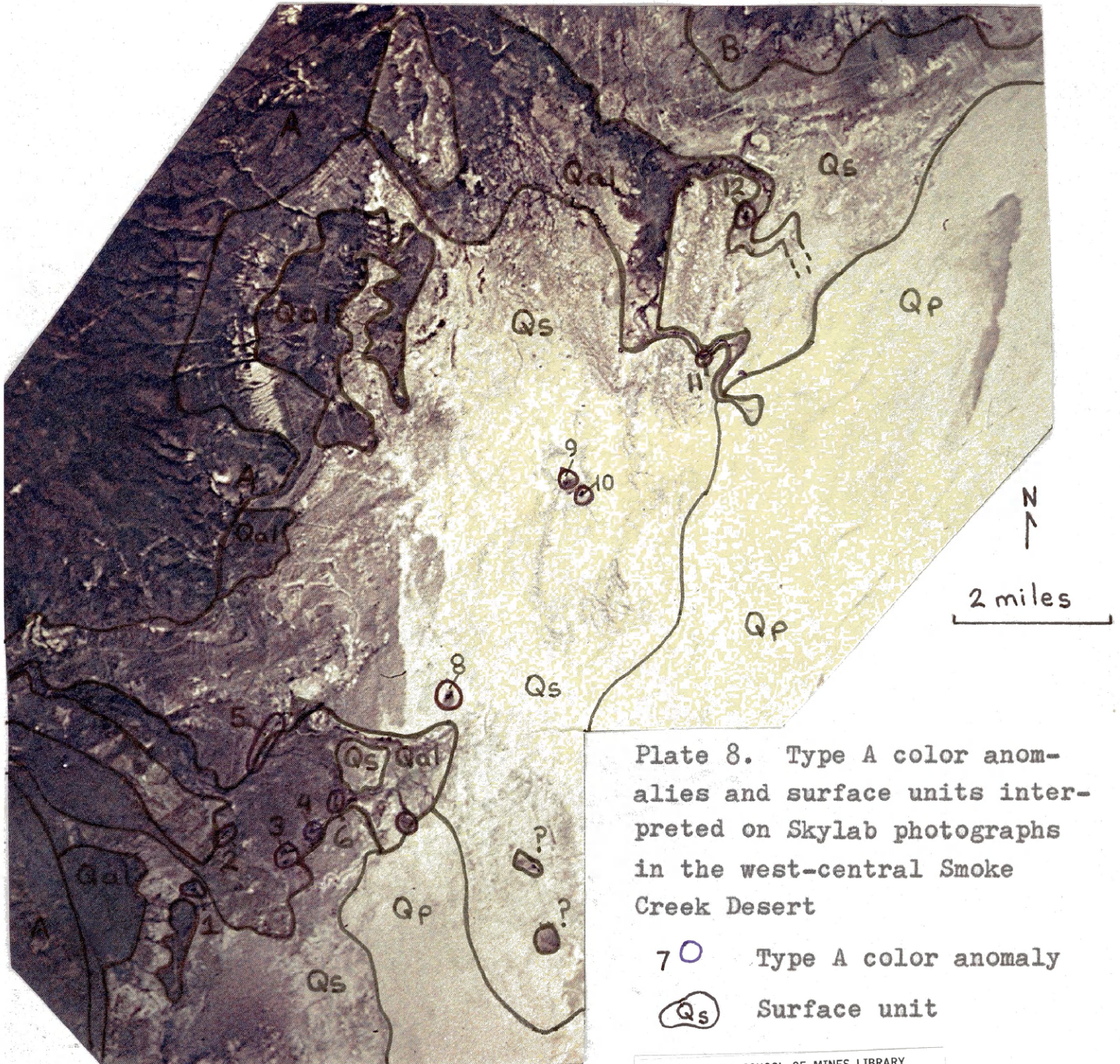
⌐‖ Type A linear

⌐ Miscellaneous
A

2 miles

N

Plate 8. Type A color anomalies and surface units interpreted on Skylab photographs in the west-central Smoke Creek Desert

7 ◯   Type A color anomaly

(Qs)   Surface unit